

# Verification and Validation of a Single-Phase Natural Circulation Loop Model in RELAP5-3D

Nicolas Zweibaum, Raluca O. Scarlat and Per F. Peterson

*University of California, Berkeley, 4118 Etcheverry Hall, MC 1730, Berkeley, CA 94720-1730*

*Email: nicolas.zweibaum@berkeley.edu*

*Submitted to the 2013 RELAP5 International Users Group Seminar*

*September 12-13, 2013*

## ABSTRACT

The University of California, Berkeley is developing best estimate fluoride-salt-cooled, high-temperature reactor (FHR) models using RELAP5-3D, and is performing integral effects experiments for code validation. As an initial validation case, a single-phase forced/natural circulation loop has been operated on the Compact Integral Effects Test (CIET) Test Bay. A model of this experimental loop has been built in RELAP5-3D, and computational results have been compared against experimental data. In this paper, the RELAP5-3D model of the experimental loop is detailed, and verification and validation efforts are presented. As part of model verification, steady-state natural circulation computational results are compared to analytical calculations for a simplified model with no heat losses along the piping, and it is shown that results from the RELAP5-3D model match analytical solutions exactly for laminar flow and reasonably for transition flow. Validation is performed using experimental data from the CIET Test Bay. Heat losses along the piping are added to the model, and mass flow rates are compared between RELAP5-3D results and experimental data. While there is a good agreement between RELAP5-3D results and experimental data for laminar flow, RELAP5-3D overpredicts natural circulation mass flow rates for transition flow. Additional validation efforts and improvements of the code are suggested to account for this effect.

## 1. INTRODUCTION

The University of California, Berkeley (UCB) is developing methods to design and perform safety analysis of fluoride-salt-cooled, high-temperature reactors (FHRs) in collaboration with the Massachusetts Institute of Technology and University of Wisconsin [1]. FHRs use a natural-circulation-driven system to passively remove decay heat from the reactor core during design basis accidents. The capability to perform verification and validation (V&V) of steady-state and transient response system models is a key issue for licensing new reactor designs. UCB is developing thermal hydraulic models to predict FHR steady-state characteristics for design optimization, and transient response during licensing basis events for safety analysis. Best estimate FHR models are developed using RELAP5-3D, and integral effects experiments are performed for code validation. As an initial validation case, a single-phase forced/natural circulation loop has been operated on the Compact Integral Effects Test (CIET) Test Bay at UCB [2]. A model of this experimental loop has been built in RELAP5-3D, and computational results have been compared against experimental data.

The CIET Test Bay is a scaled height, reduced flow area loop, which reproduces the integral thermal hydraulic response of the FHR primary coolant flow circuit by using Dowtherm A oil as a low-temperature simulant fluid for the prototypical fluoride salt coolants. On the CIET Test Bay, heat is added to the fluid through an annular, electrically-heated pipe, and removed through water-cooled heat exchangers. Mass flow rates and bulk fluid temperatures along the loop are collected at various levels of heat input. The RELAP5-3D model of the loop reproduces its geometry, temperature and pressure boundary conditions, as well as working fluid thermophysical properties as implemented in the code [3]. The CIET Test Bay is described here, and details of the RELAP5-3D model of the natural circulation loop are provided.

As part of model verification, steady-state natural circulation computational results are compared to analytical calculations for a simplified model with no heat losses along the piping, where such solutions exist for mass flow rate and temperature rise across the heat source, based on heat input, loop geometry and average fluid properties. Mass flow rate is the main metric of interest throughout this study, since higher mass flow rates mean more effective natural circulation heat removal from the system. Sensitivities to

initial and boundary conditions, as well as model discretization, are also assessed.

Validation is performed using experimental data from the CIET Test Bay. Heat losses along the piping are added to the computational model, and mass flow rates are compared between RELAP5-3D results and experimental data for given heat inputs. Because of limitations to the temperature range of Dowtherm A thermophysical properties in RELAP5-3D, the actual experimental boundary conditions cannot be modeled. However, validation of steady-state models is performed by comparing RELAP5-3D results to experimental data in the non-dimensional space.

As a result of this study, suggestions are made to improve the code in order to better simulate natural circulation with transition flow. An extended experimental plan is also presented to complete the V&V efforts introduced here.

## 2. CIET TEST BAY EXPERIMENTAL CONFIGURATION AND RELAP5-3D MODEL

The CIET Test Bay geometry, boundary conditions and instrumentation are introduced here, so that one can use the collected experimental data as a benchmark for other studies. Details about the RELAP5-3D model of the loop are also provided, and an example input deck is included as an Appendix.

### 2.1. CIET Test Bay Natural Circulation Loop

The CIET Test Bay is a natural circulation loop using simulant fluids for the class of liquid salts considered in the baseline design of FHRs. The fluid used is a heat transfer oil, commercially available under the name of Dowtherm A or Therminol VP. The loop consists of a vertical annular heated section, a vertical straight pipe heat exchanger with four parallel branches, and the connected piping. The hot leg is the piping connecting the top of the heater to the top of the heat exchanger. The cold leg is the piping connecting the bottom of the heat exchanger to the bottom of the heater. Figure 1 shows front and side views of the Test Bay, and Table 1 gives the physical dimensions of each segment. More details can be found in [2].

All parts of the loop are made of copper piping, except for the stainless steel annular heated section. This section is electrically heated using a varying power supply in the range of 0 to 10 kW, connected to the heater outer tube through copper electrodes. The heat exchanger is a coaxial

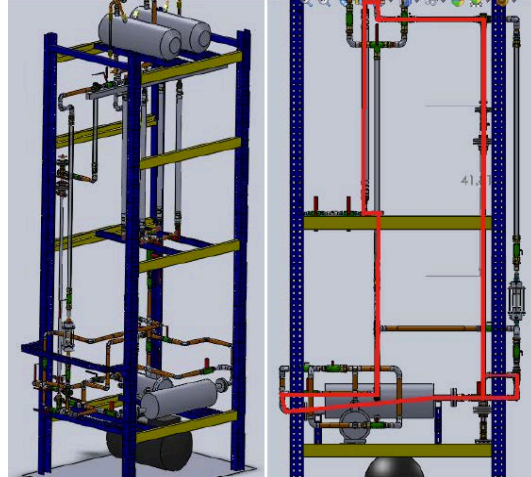


Figure 1. CIET Test Bay front view (left), and side view showing natural circulation flow path (right) (SolidWorks model by A.J. Gubser, UCB) [2].

Table 1. Physical parameters of the natural circulation loop (all dimensions given in m).

<b>Elevation Change</b>	
Heated Section	1.4605
Hot Leg	0.8397
Cooled Section	-1.0110
Cold Leg	-1.2892
Buoyancy Head	1.0645
<b>Heated Section</b>	
OD of Annulus	0.01827
ID of Annulus	0.01441
Annulus Length	1.7811
Heated Length	1.4605
<b>Piping</b>	
Pipe Diameter	0.0268
Length of Hot Leg	3.3472
Length of Cold Leg	2.3695
<b>Cooled Section</b>	
Pipe Diameter	0.0206
Length	1.6956
Cooled Length	1.0110

cylindrical copper heat exchanger with 10°C water flowing into the annulus. The high value of the water flow rate minimizes the temperature difference between the water inlet and outlet, and the temperature difference between the copper inner tube and the water. All parts of the loop are covered with 5-cm-thick fiberglass insulation to limit heat losses to the ambient air, except for the heat exchanger. An expansion tank with atmospheric pressure boundary is installed at the uppermost elevation of the loop, to allow for

volumetric expansion of the fluid. It is thus assumed that the boundary conditions are:

- Adiabatic on the stainless steel inner tube of the annular heater,
- Uniform heat flux to solid on the stainless steel outer tube of the annular heater,
- Copper piping with 5-cm-thick fiberglass insulation on the hot and cold legs,
- 10°C uniform temperature on the outer wall of the inner heat exchanger tube,
- 20°C ambient temperature around the rest of the loop,
- 101.33 kPa pressure at the free surface of the expansion tank.

The loop is instrumented with type-T inline thermocouples (TCs) with 0.5-mm-diameter sheaths and ungrounded junctions (Omega Engineering part number TMTSS-020U-6) to measure bulk fluid temperatures at the inlet and outlet of the heater, and at the inlet and outlet of the heat exchanger. The TCs are calibrated against National Institute of Standards and Technology-calibrated resistance temperature detector probes. Calibration was performed after all the wiring connections were installed, and before the TCs were installed on the experimental loop. The type-T TCs accuracy is  $\pm 0.8^\circ\text{C}$  in the 0-200°C range. The TCs are connected to a National Instruments SCXI-1102 data acquisition module.

Mass flow rates are directly measured using a Coriolis flowmeter (Siemens MASS 2100 DI 25 sensor). The error is given by the vendor as:

$$E = \pm \sqrt{(0.10)^2 + \left(\frac{Z \cdot 100}{qm}\right)^2} \quad (2.1)$$

where:

$E$  [%] is the error on mass flow rate,  
 $Z$  [kg/h] is the zero point error,  
 $qm$  [kg/h] is the mass flow rate.

For each run, the heat input is set through the power supply controls. The power supply (TDK-Lambda GENESYS 10 kW programmable DC power supply) has accuracies of  $\pm 0.5\%$  on both voltage and current outputs, resulting in a  $\pm 1\%$  accuracy on power output.

To collect the data used in this study, temperatures and mass flow rate in the loop are recorded when steady-state conditions have been reached.

## 2.2. CIET Test Bay RELAP5-3D Model

The RELAP5-3D model of the CIET Test Bay reproduces its geometry, pressure boundary condition and working fluid thermophysical properties as implemented in the code. The 20°C ambient temperature is also matched. However, because thermophysical properties of Dowtherm A have not been implemented in RELAP5-3D for temperatures below 25°C around atmospheric pressure [3], the lower limit on the heat exchanger outer wall temperature is 25°C, and experimental conditions cannot be matched in the code. Material properties for the copper and stainless steel piping, as well as the fiberglass insulation, are manually implemented in the model. A diagram of the RELAP5-3D model of the CIET Test Bay is provided in Figure 2, and the type and geometry for each component in the model are listed in Table 2.

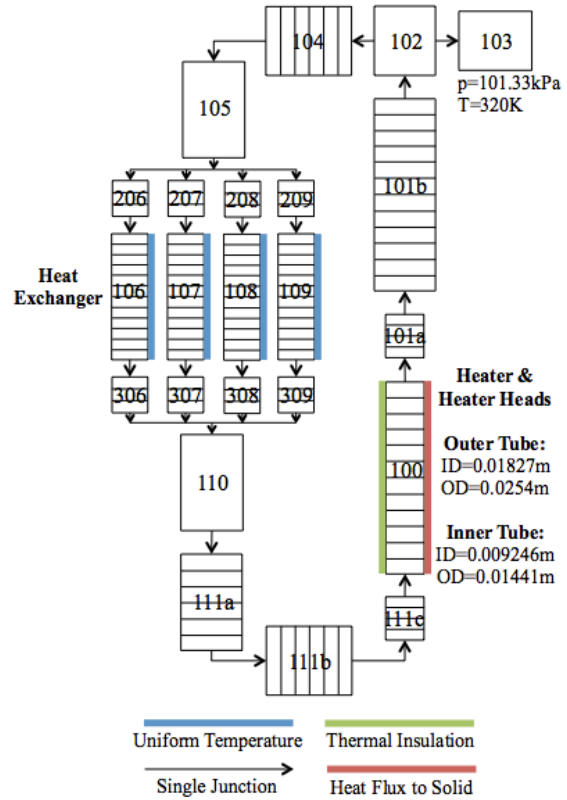


Figure 2. Nodalization of CIET Test Bay simplified model in RELAP5-3D.

Figure 2 shows the diagram for a model of the Test Bay where no heat structures are attached to the hot leg and cold leg piping. This model, referred to as “simplified model” in this study, is used for verification purposes. The model including heat structures attached to the hot leg and cold leg

pipings with insulation is referred to as “full model”. The segments on each pipe represent incremental control volumes and associated heat structures (sensitivity to the discretization of the model is discussed below).

Parameters for the heat structures attached to the heater inner tube, outer tube and the heat exchanger in the simplified model, as well as the hot and cold legs in the full model, are provided in Table 3. Because the heater is an annular section with heat input to the outer tube only, the heated equivalent diameter, defined as

$4 \left( \frac{\text{flow area}}{\text{heated perimeter}} \right)$ , is greater than the volume hydraulic diameter, and therefore explicitly included in the model, as suggested in the RELAP5-3D user manual [4]. Three radial mesh points are used in the full model for the pipe wall and fiberglass insulation regions (2 mesh points for each).

For this study, all calculations are run with RELAP5-3D/Ver. 4.0.3 in transient mode until steady-state conditions are reached for fluid temperatures and mass flow rate around the loop.

Table 2. List of component types and parameters in the RELAP5-3D model of the CIET Test Bay (the numbers correspond to the diagram in Figure 2).

Component	Type	Number	Length [m]	Hydraulic Diameter [m]	Flow Area [m <sup>2</sup> ]
Heater	pipe	100	1.4605	3.86E-3	9.907E-5
Heater Heads	pipe	101a, 111c	0.1603	3.86E-3	9.907E-5
Hot Leg 1	pipe	101b	1.5265	0.0268	5.640E-4
Branch	branch	102	0.0268	0.0268	5.640E-4
Tank	tmdpvol	103	1.0	N/A	1.0
Hot Leg 2	pipe	104	0.7597	0.0268	5.640E-4
HX Branch	branch	105, 110	0.5316	0.0268	5.640E-4
HX	pipe	106-9	1.0110	0.0206	3.333E-4
HX Heads	pipe	206-9, 306-9	0.3423	0.0206	3.333E-4
Cold Leg 1	pipe	111a	0.5756	0.0268	5.640E-4
Cold Leg 2	pipe	111b	0.7597	0.0268	5.640E-4

Table 3. List of heat structures and parameters in the RELAP5-3D model of the CIET Test Bay.

Component	Number	Radial Mesh Points	Boundary Condition Type		Heated Equivalent Diameter [m]		Wall Thickness [m]
			Left	Right	Left	Right	
Heater Outer Tube	100-1	2	Convection	Adiabatic	6.90E-3	N/A	See Fig. 2 Legend
Heater Inner Tube	100-2	2	Adiabatic	Convection	N/A	8.75E-3	See Fig. 2 Legend
HX	106-9	2	Convection	Fixed T	N/A	N/A	8.13E-4
<i>Full Model Only</i>							
Heater Heads (Outer)	101a-1, 111c-1	3	Convection	Fixed T	6.90E-3	N/A	See Fig. 2 Legend
Heater Heads (Inner)	101a-2, 111c-2	2	Adiabatic	Convection	N/A	8.75E-3	See Fig. 2 Legend
Hot Leg 1	101b	3	Convection	Fixed T	N/A	N/A	8.89E-4
Branch	102	3	Convection	Fixed T	N/A	N/A	8.89E-4
Hot Leg 2	104	3	Convection	Fixed T	N/A	N/A	8.89E-4
HX Branch	105, 110	3	Convection	Fixed T	N/A	N/A	8.89E-4
HX Heads	206-9, 306-9	3	Convection	Fixed T	N/A	N/A	8.13E-4
Cold Leg	111a, b	3	Convection	Fixed T	N/A	N/A	8.89E-4

### 3. SOLUTION AND CODE VERIFICATION FOR NATURAL CIRCULATION

As highlighted by Oberkampf and Trucano, verification is “the process of determining that a model implementation accurately represents the developer’s conceptual description of the model and the solution to the model” [5]. The authors divide the verification effort between solution verification, assessing the numerical accuracy of the solution to a computational model, and code verification, assessing the reliability of the software coding. Such efforts are pursued here, to the extent made possible for end users of the executable version of the RELAP5-3D code.

#### 3.1. Fluid Thermophysical Properties

All analytical solutions calculated as part of the verification process use the following temperature-dependent thermophysical properties for Dowtherm A, based on data in the 20-180°C range [6]:

$$\mu = \frac{0.130}{T^{1.072}} \quad (3.1)$$

$$c_p = 1518 + 2.82 \cdot T \quad (3.2)$$

$$k = 0.142 - 0.00016 \cdot T \quad (3.3)$$

$$\rho = 1078 - 0.85 \cdot T \quad (3.4)$$

where:

$T$  [°C] is the fluid temperature,

$\mu$  [Pa · s] is the fluid dynamic viscosity,

$c_p$  [J/kg°C] is the fluid specific heat capacity,

$k$  [W/m°C] is the fluid thermal conductivity,

$\rho$  [kg/m<sup>3</sup>] is the fluid density.

It has been verified that Dowtherm A thermophysical properties at atmospheric pressure implemented in RELAP5-3D lie within ±0.4% of the values obtained with Eq. 3.1-4 in the 20-180°C temperature range [3].

#### 3.2. Solution Verification

For solution verification purposes, sensitivity of the natural circulation mass flow rate to a set of initial and boundary conditions, as well as model discretization, is assessed in RELAP5-3D. This sensitivity analysis is performed using the CIET Test Bay simplified model presented in Figure 2 as a reference, with 1 kW heat input. The results are

summarized in Table 4, where solutions are reported as *not sensitive* to a parameter when they vary by less than 0.1% for any value of the parameter.

Table 4. Sensitivity of natural circulation mass flow rate calculated by RELAP5-3D to a set of model parameters.

Model Input Parameter	Parameter Range	Sensitivity of Solution
Expansion tank temperature [°C]	25 – 180	Not sensitive
Loop initial temperature [°C]	25 – 180	Not sensitive
Loop initial pressure [kPa]	100 – 200	Not sensitive
Loop initial mass flow rate [kg/s]	0.01 – 1	Not sensitive
Form losses	0 – 10	Not sensitive
Wall radial discretization [number of meshes]	2 – 20	Not sensitive
Hot leg and cold leg axial discretization [number of control volumes]	10 – 50	Not sensitive
Heater and heat exchanger axial discretization [number of control volumes]	6 – 60	Sensitive

As expected, the steady-state natural circulation mass flow rate is not sensitive to the expansion tank fixed temperature, since at steady-state, there is no flow going in or out of the tank. It is not sensitive to initial conditions, which should not impact steady-state behavior of the loop. It is not sensitive to form losses from elbows or tees in the loop, since pressure drops in the laminar and transition regimes are largely dominated by friction losses along the piping. It is not sensitive to radial discretization of the walls because the temperature distribution there is approximately linear, nor to axial discretization of the hot and cold leg because these are adiabatic. However, because of significant temperature gradients, the steady-state mass flow rate calculated by RELAP5-3D is sensitive to axial discretization of the heater and heat exchanger, as shown in Figure 3.

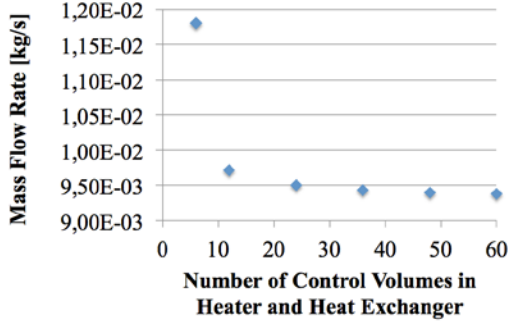


Figure 3. Sensitivity of natural circulation mass flow rate to axial discretization of heater and heat exchanger in RELAP5-3D.

Figure 3 shows that RELAP5-3D solutions converge for a number of control volumes above 30 for the heater and heat exchanger (mass flow rate varies by less than 0.5% for any higher number of control volumes). Therefore, a conservative number of 60 control volumes for the heater and heat exchanger is used for subsequent models of the CIET Test Bay.

### 3.3. Code Verification

For code verification purposes, computational results of the CIET Test Bay simplified model in RELAP5-3D are compared to analytical results in the heat input range of interest (1-10 kW, with 1 kW increments).

As a first code verification step, the following tests are performed:

- Is the heat input to the fluid equal to the heat removed through the heat exchanger at steady-state?
- Are temperatures uniform along the adiabatic hot leg and cold leg?
- Is the mass flow rate uniform along the loop?
- Is the following equation verified:

$$Q_h = \dot{m} c_{p,av} \Delta T_h \quad (3.5)$$

where:

$Q_h [W]$  is the heat input from the heater,  
 $\dot{m} [kg/s]$  is the loop mass flow rate,  
 $c_{p,av} [J/kg^\circ C]$  is the average specific heat capacity of the fluid in the heater,  
 $\Delta T_h [^\circ C]$  is the temperature change of the fluid across the heater.

The code results have passed these tests, hence partly verifying proper solving of the fundamental conservation equations.

Scarlat has derived the following expression from the mass, momentum and energy conservation

equations for natural circulation mass flow rate, based on fluid average thermophysical properties and loop geometry [2]:

$$\dot{m}^3 = \frac{2\rho_{av}^2 g \beta}{c_{p,av}} \cdot \frac{\Delta z_{NC} Q_h}{F'} \quad (3.6)$$

$$F' = \sum_{i=1}^N \left( \frac{1}{A_i^2} \cdot \frac{L_i}{D_i} \right) f_i \quad (3.7)$$

where:

$\rho_{av} [kg/m^3]$  is the average density of the fluid,  
 $g [m/s^2]$  is the gravity constant,  
 $\beta [^\circ C^{-1}]$  is the average volumetric expansion coefficient of the fluid,  
 $\Delta z_{NC} [m]$  is the buoyancy head, defined as the elevation difference between the centerlines of the heated and cooled sections,  
 $A_i [m^2]$  is the cross-sectional area of section  $i$ ,  
 $L_i [m]$  is the length of section  $i$ ,  
 $D_i [m]$  is the hydraulic diameter of section  $i$ ,  
 $f_i$  is the friction factor in section  $i$ ,  
 $N$  is the total number of sections in the loop.

Equation 3.6 is implicit since  $f_i$  depends on  $Re_i$ , the Reynolds number in section  $i$ , which in turns depends on  $\dot{m}$  through:

$$Re_i = \frac{1}{\mu_i} \dot{m} \frac{D_i}{A_i} \quad (3.8)$$

where  $\mu_i [Pa \cdot s]$  is the dynamic viscosity of the fluid in section  $i$ . However, using the following expressions for  $f_i$ , Eq. 3.6 can be solved [7]:

$$f = \frac{64}{Re} \text{ for } 0 < Re < 2000 \quad (3.9)$$

$$f = \frac{Re^{1/3}}{381} \text{ for } 2000 < Re < 4000 \quad (3.10)$$

Analytical solutions of Eq. 3.6, using Eq. 3.9 in laminar regime and Eq. 3.10 in transition regime, are compared to RELAP5-3D solutions. Results are shown in Figure 4. Since Eq. 3.6 uses average fluid thermophysical properties, analytical results are calculated, for various heat inputs, at the average, minimum and maximum fluid temperatures obtained from RELAP5-3D (labeled ‘‘Analytical, T from RELAP5-3D,’’ ‘‘Analytical, T Low’’ and ‘‘Analytical, T High,’’ respectively).

In this heat input range, the agreement between RELAP5-3D results and analytical solutions using the average fluid temperature obtained from RELAP5-3D is within 5% in the laminar regime and within 8% in the transition regime. The

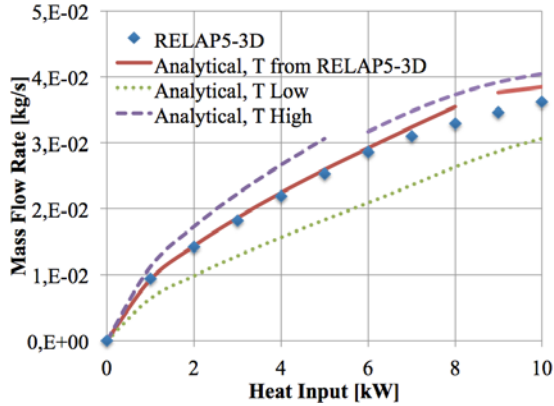


Figure 4. Comparison of analytical and RELAP5-3D solutions of natural circulation mass flow rate for various heat inputs.

discrepancy between analytical and RELAP5-3D results in the transition regime can essentially be explained by RELAP5-3D using an interpolation different from Eq. 3.10 between the fully laminar friction factor (Eq. 3.9) and the fully turbulent friction factor [8]. The small discrepancy between analytical and RELAP5-3D results in the high end of the laminar regime (heat input higher than 6 kW) can probably be explained by the temperature-dependent thermophysical properties used in RELAP5-3D, while Eq. 3.6 uses average fluid thermophysical properties. However, RELAP5-3D solutions lie between the low and high ends of analytical solutions for mass flow rate throughout the 0-10 kW heat input range.

For code verification, sensitivity of the natural circulation mass flow rate to the heat exchanger outer wall uniform temperature boundary condition is also assessed. Indeed, higher temperature boundary conditions lead to a higher average fluid temperature in the loop at steady-state, which is expected to lead to higher mass flow rates based on Eq. 3.6. This result is shown in Figure 5, where mass flow rates are obtained with RELAP5-3D for heat exchanger outer wall temperatures in the range of 25-70°C.

As expected, mass flow rates are highly sensitive to heat exchanger surface temperature, thus confirming the necessity to properly account for the impact of this boundary condition on natural circulation problems solved with RELAP5-3D.

### 3.4. Conclusions of the Verification Effort

In the heat input range of interest, the agreement between RELAP5-3D results and analytical solutions is within 5% in the laminar regime and within 8% in the transition regime for simplified natural circulation models. Moreover,

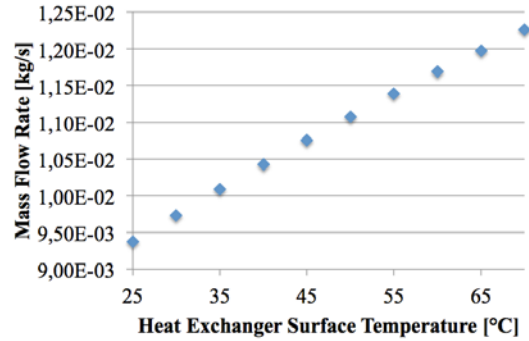


Figure 5. Natural circulation mass flow rate calculated by RELAP5-3D for various heat exchanger outer wall temperatures.

RELAP5-3D solutions lie between the low and high values of analytical solutions for mass flow rate throughout this range. The model has been developed to a point where it is only sensitive to relevant physical parameters for our application, such as heat input to the fluid and heat exchanger temperature boundary conditions. The discrepancies observed between RELAP5-3D and analytical solutions, essentially in the transition regime, may be due to the use of average fluid thermophysical properties in Eq. 3.6 for analytical solutions, and to the use of different friction factor correlations in the transition flow region. The latter effect is further analyzed through the validation phase of the V&V effort.

## 4. MODEL VALIDATION

Oberkampf and Trucano define validation as “the process of determining the degree to which a model is an accurate representation of the real world from the perspective of the intended uses of the model” [5]. This is done here by comparing the computational results from RELAP5-3D to experimental data from the CIET Test Bay.

### 4.1. CIET Test Bay Experimental Data

A series of runs has been performed on the CIET Test Bay, where mass flow rates and temperatures of the fluid in the natural circulation loop have been recorded at steady-state for various heat inputs. A summary of the collected data is provided in Table 5.

### 4.2. Model Calibration

There is a clear distinction between model validation and calibration efforts, where validation is an assessment of the model in a “blind” test with

experimental data, whereas the key issue in calibration is to adjust the physical modeling parameters to improve agreement with experimental data [5]. In this case, as part of the calibration effort, because the exact dimensions of the annular heated element as a result of thermal expansion are not known for each data point listed in Table 5, these dimensions have been back-calculated from pressure drop measurements across the heater based on analytical calculations [2], and the back-calculated dimensions, listed in Figure 2, are used in the RELAP5-3D model of the heater.

#### 4.3. Direct Comparison of RELAP5-3D Results to Experimental Data

The RELAP5-3D full model of the CIET Test Bay is run at the various power levels listed in Table 5. Because the lower limit on the heat exchanger outer wall temperature is 25°C, and because natural circulation mass flow rate is approximately linear with heat exchanger surface temperature as shown in Figure 4, mass flow rates obtained with RELAP5-3D for higher heat exchanger outer wall temperatures are linearly extrapolated to values for a 10°C uniform heat exchanger wall temperature. Results are shown in Figure 6, where two data points have large uncertainty bands due to high zero point errors on the flowmeter for these specific runs (see Eq. 2.1).

At low heat inputs (left of Figure 6), the agreement between RELAP5-3D results and experimental data is within 10%, and RELAP5-3D solutions lie inside the uncertainty bands of the data, showing an excellent agreement with experimental values. At higher heat inputs (right of Figure 6), the major trend of the data is correctly predicted by RELAP5-3D, the agreement between RELAP5-3D results and experimental data is within 20%, and the calculation results lie outside

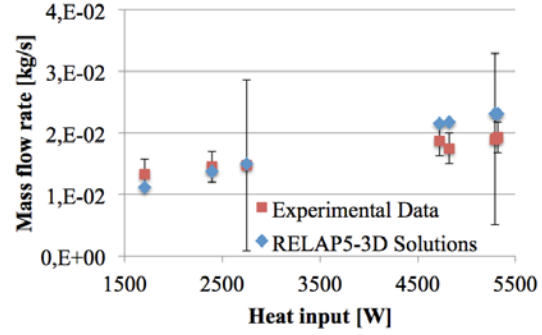


Figure 6. Comparison of experimental and RELAP5-3D natural circulation mass flow rates for various heat inputs.

but near the uncertainty bands of the data. However, the observed overprediction of mass flow rate for a given heat input is not conservative for this application, since higher mass flow rates mean more effective heat removal from the system, which is its primary passive safety goal.

#### 4.4. Non-Dimensional Comparison of RELAP5-3D Results to Experimental Data

The direct comparison shown in Figure 6 is not optimal since it results from an extrapolation of the RELAP5-3D solutions to experimental boundary conditions. Vijayan proposes a non-dimensional, generalized correlation of the following form for steady flow in a fully laminar or fully turbulent natural circulation loop [9]:

$$Re = C \left[ \frac{(Gr_m)_{\Delta z_{NC}}}{N_G} \right]^r \quad (4.1)$$

$$Re = \frac{D_r \dot{m}}{A_r \mu_{av}} \quad (4.2)$$

Table 5. Experimental data from CIET Test Bay.

Power [W]	Mass flow rate [kg/s]	Error on mass flow rate [kg/s]	Heater average T [°C]	Heater $\Delta T$ [°C]	Error on heater $\Delta T$ [°C]	Heat exchanger $\Delta T$ [°C]	Hot leg $\Delta T$ [°C]	Cold leg $\Delta T$ [°C]
1707	1.33E-02	2.5E-03	74.0	79.2	1.2	-87.6	-2.8	11.1
2396	1.45E-02	2.5E-03	76.9	99.0	1.5	-89.1	-14.0	4.0
2748	1.47E-02	1.4E-02	86.4	100.4	1.5	-84.4	-25.9	9.8
4725	1.88E-02	2.5E-03	111.0	138.7	2.1	-128.2	-16.5	5.9
4821	1.75E-02	2.5E-03	104.4	154.6	2.3	-128.9	-22.2	-3.5
5295	1.90E-02	1.4E-02	116.0	148.0	2.2	-137.0	-15.0	4.0
5317	1.93E-02	2.5E-03	114.5	152.5	2.3	-136.1	-18.1	1.7

$$(Gr_m)_{\Delta z_{NC}} = \frac{D_r^3 \rho_{av}^2 \beta_{av} g Q_h \Delta z_{NC}}{A_r \mu_{av}^3 c_{p,av}} \quad (4.3)$$

$$N_G = \frac{L_t}{D_r} \sum_{i=1}^N \left( \frac{l_{eff}}{d^{1+b} a^{2-b}} \right)_i \quad (4.4)$$

where:

$$L_t = \sum_{i=1}^N L_i,$$

$$D_r = \frac{1}{L_t} \sum_{i=1}^N D_i L_i,$$

$$A_r = \frac{1}{L_t} \sum_{i=1}^N A_i L_i,$$

$$d_i = \frac{D_i}{D_r},$$

$$a_i = \frac{A_i}{A_r},$$

$$(l_{eff})_i = (L_{eff})_i / L_t,$$

$$(L_{eff})_i = L_i + Le_i,$$

$$Le_i = \frac{K_i D_i}{f_i},$$

$K_i$  is the sum of form loss coefficients in section  $i$ .

The correlation is applicable if a friction law of the form  $f = \frac{p}{Re^b}$  is valid throughout the loop with the same values of  $p$  and  $b$ . Then, Vijayan shows that:

$$C = \left( \frac{2}{p} \right)^r \quad (4.5)$$

$$r = \frac{1}{3-b} \quad (4.6)$$

For fully laminar flow ( $p = 64$ ,  $b = 1$ ),  $C = 0.1768$  and  $r = 0.5$ . For fully transition flow,  $C = 1.216$  and  $r = 0.387$ .

Results of the comparison between RELAP5-3D calculations and experimental data in the non-dimensional space, following the form of Eq. 4.1, are shown in Figure 7. Figure 7 uses a logarithmic scale in order to show a linear trend, based on the predicted form of the correlation in Eq. 4.1.

At low values of  $(Gr_m)_{\Delta z_{NC}}$  (corresponding to low heat inputs), the agreement between RELAP5-3D results and experimental data is within 10%, and RELAP5-3D solutions lie inside the uncertainty bands of the data, showing an excellent agreement with experimental values. At higher heat inputs, the major trend of the data is correctly predicted by RELAP5-3D, the agreement between RELAP5-3D results and experimental data is within 25%, and the

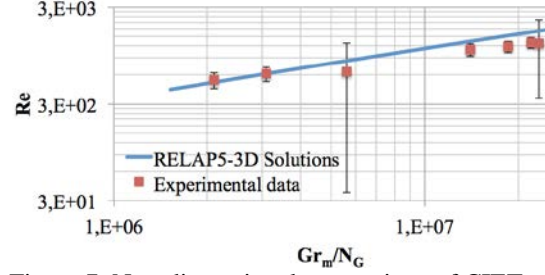


Figure 7. Non-dimensional comparison of CIET Test Bay experimental data and RELAP5-3D natural circulation model.

calculation results lie outside but near the uncertainty bands of the data. However, RELAP5-3D tends to overpredict mass flow rate for a given heat input, which is not conservative for our end application of passive decay heat removal system modeling for the FHR.

#### 4.5. Conclusions of the Validation Effort

Limitations to the thermophysical properties of Dowtherm A as implemented in RELAP5-3D do not allow for a direct comparison of RELAP5-3D calculations to experimental data collected on the CIET Test Bay. However, Eq. 4.1 provides a means to properly compare RELAP5-3D solutions to the data in the non-dimensional space. This comparison shows an excellent agreement between the code calculations and the experimental data at low heat inputs, where the loop is in fully laminar flow, and an overprediction of natural circulation mass flow rates by the code at higher heat inputs, where the loop is in transition flow. Swapnalee and Vijayan have derived an empirical correlation for transition regime friction factors [10]:

$$f = \frac{1.2063}{Re^{0.416}} \quad (4.7)$$

This correlation is valid for  $898 < Re < 3196$ , where the transition regime for natural circulation loops starts at lower values of Reynolds number than the general 2000 value shown in Eq. 3.9 and Eq. 3.10. This friction factor correlation, based on experimental data, is higher than most correlations found in the literature for transition flow, and leads to lower steady-state mass flow rates. This could be the main explanation to the observed discrepancy between RELAP5-3D calculations and the CIET Test Bay data, however, the executable version of RELAP5-3D does not allow the user to

specify alternate friction factor correlations in the laminar regime, preventing us from testing this hypothesis.

## 5. CONCLUSIONS AND FUTURE WORK

This V&V study shows that, under some conditions, RELAP5-3D is an appropriate tool to model the CIET Test Bay, as a first step towards predicting the performance of the passive decay heat removal system of FHRs. The code shows agreement within 5% with analytical pre-predictions and within 10% with experimental data for natural circulation in the laminar regime, and it shows agreement within 8% with analytical solutions and within 25% with experimental data in the transition regime. However, RELAP5-3D tends to overpredict natural circulation mass flow rates in the transition regime compared to both analytical solutions and experimental data, which is probably due to a discrepancy between the friction factor correlations as implemented in the code and what they actually are in the experimental loop. This could be an issue if one were to predict the performance of the passive decay heat removal of the FHR using RELAP5-3D, because at high decay heat levels, where the coolant flow is in transition regime, the efficiency of heat transfer in the loop could be overestimated.

Because the current validation effort only uses 7 experimental data points, with some high uncertainties in the measured mass flow rates, the next step will be to continue the study with additional data. The current data set could then serve as a calibration basis to make pre-predictions of the behavior of the loop for future runs. Collecting additional data will also help to ensure that the non-dimensional space boundaries in which validation is performed include the expected operational states of the FHR, allowing to use RELAP5-3D to predict the performance of the passive decay heat removal system of the reactor. Finally, and most importantly, because it is recognized that the inaccuracy of the RELAP5-3D solutions in the transition regime is probably due to the friction factor correlations built into the code, this study is a strong incentive for allowing the end user to modify these correlations, not only in the turbulent regime as it is currently the case, but also in the laminar and transition regimes.

## 6. ACKNOWLEDGEMENT

This research was performed using funding received from the U.S. Department of Energy Office of Nuclear Energy's Nuclear Energy University Programs. The authors would also like to thank Dr. Cliff B. Davis, from the Idaho National Laboratory, for his precious advice during the development of the models used for this study.

## 7. REFERENCES

1. C. FORSBERG, L.W. HU, P.F. PETERSON, and K. SRIDHARAN, "Fluoride-Salt-Cooled High-Temperature Reactors for Base-Load and Peak Electricity, Grid Stabilization, and Process Heat," MIT-ANP-TR-147, Department of Nuclear Science and Engineering, Massachusetts Institute of Technology (2013).
2. R.O. SCARLAT, "Design of Complex Systems to Achieve Passive Safety: Natural Circulation Cooling of Liquid Salt Pebble Bed Reactors," PhD Dissertation, Department of Nuclear Engineering, University of California, Berkeley (2012).
3. R.L. MOORE, "Implementation of Dowtherm A Properties into RELAP5-3D/ATHENA," INL/EXT-10-18651, Idaho National Laboratory (2010).
4. The RELAP5-3D Code Development Team, "RELAP5-3D Code Manual Volume II: User's Guide and Input Requirements," INEEL-EXT-98-00834, Revision 4.0, Idaho National Laboratory (2012).
5. W.L. OBERKAMPF AND T.G. TRUCANO, "Verification and Validation Benchmarks," Nuclear Engineering and Design, 238, 716–743 (2008).
6. The Dow Chemical Company, "Dowtherm A Heat Transfer Fluid Product Technical Data" (1997).
7. R.A. SEBAN AND J.A. HODGSON, "Laminar Film Condensation in a Tube with Upward Vapor Flow," International Journal of Heat and Mass Transfer, 25, 1291–1299 (1982).
8. The RELAP5-3D Code Development Team, "RELAP5-3D Code Manual Volume I: Code Structure, System Models and Solution Methods," INEEL-EXT-98-00834, Revision 4.0, Idaho National Laboratory (2012).

9. P.K. VIJAYAN, “Experimental Observations on the General Trends of the Steady State and Stability Behaviour of Single-Phase Natural Circulation Loops,” *Nuclear Engineering and Design*, 215, 139–152 (2002).
10. B.T. SWAPNALEE AND P.K. VIJAYAN, “A Generalized Flow Equation for Single Phase Natural Circulation Loops Obeying Multiple Friction Laws,” *International Journal of Heat and Mass Transfer*, 54, 2618–2629 (2011).

**APPENDIX: EXAMPLE RELAP5-3D CIET TEST BAY MODEL (INPUT DECK)**

=Natural Circulation in CIET Test Bay  
\* HX surface T=25°C; P=1.707kW; ambient T=20°C  
\* Heater dimensions back-calculated from dp measurements  
\* 3in fiberglass insulation (except on HX)  
\* 60 control volumes for heater and heat exchangers  
\* New problem using non-standard fluid; transient mode  
100 newath transnt  
\* SI units for input; SI units for output  
102 si si  
\* Reference volume; reference elevation; fluid (Dowtherm A)  
120 100010000 0.0000 dowa  
\* End time; min time step; max time step; control option;  
\* Minor edit frequency; major edit frequency; restart frequency  
201 2000.000 1.0e-7 0.1 15011 1 1000 1000  
202 20000.00 1.0e-6 1.0 15011 5 1000 1000  
\*  
\*\*\*\*\*  
\* Hydrodynamic components  
\*\*\*\*\*  
\*  
\* Heater  
\* Component name; component type  
1000000 heater pipe  
\* Number of elements  
1000001 60  
\* Volume flow area; which elements  
1000101 9.9074e-5,60  
\* Volume length; which elements  
1000301 0.024342,60  
\* Volume azimuthal angle; which elements (optional card)  
1000501 0.0,60  
\* Volume inclination angle; which elements (required)  
1000601 90.0,60  
\* Wall roughness; hydraulic diameter; which elements  
\* Here for stainless steel: k=0.015mm  
1000801 1.5e-5,3.860e-3,60  
\* tlpvbf (see p.113 of Manual Appendix A); which elements  
1001001 0,60  
\* jefvcahs (see p.115 of Manual Appendix A); which elements  
1001101 0,59

\* ebt (initial conditions options); P; T; 0; 0; 0; which elements  
1001201 3,1.6e5,325.0,0.,0.,0.,60  
\* Junction initial conditions control option  
\* 0 for velocities, 1 for mass flow rates  
1001300 1  
\* Initial liquid velocity; initial gas velocity;  
\* Interface velocity (enter 0.0); junction number  
1001301 0.010,0.010,0.,59  
\*  
\* Hot leg 1  
\* Component name; component type  
1010000 hotleg1 pipe  
\* Number of elements  
1010001 16  
\* Volume flow area; which elements  
1010101 9.9074e-5,4  
1010102 5.640e-4,16  
\* Volume length; which elements  
1010301 4.00625e-2,4  
1010302 0.12721,16  
\* Volume azimuthal angle; which elements (optional card)  
1010501 0.0,16  
\* Volume inclination angle; which elements (required)  
1010601 90.0,16  
\* Wall roughness; hydraulic diameter; which elements  
\* Here for stainless steel: k=0.015mm; copper: k=0.0015mm  
1010801 1.5e-5,3.860e-3,4  
1010802 1.5e-6,2.680e-2,16  
\* tlpvbf (see p.113 of Manual Appendix A); which elements  
1011001 0,16  
\* jefvcahs (see p.115 of Manual Appendix A); which elements  
1011101 0,3  
1011102 100,4 \* Abrupt area change  
1011103 0,15  
\* ebt (initial conditions options); P; T; 0; 0; 0; which elements  
1011201 3 1.5e5,325.0,0.,0.,0.,16  
\* Junction initial conditions control option  
\* 0 for velocities, 1 for mass flow rates  
1011300 1  
\* Initial liquid velocity; initial gas velocity;  
\* Interface velocity (enter 0.0); junction number  
1011301 0.010,0.010,0.,15  
\*  
\* Expansion tank  
\* Component name; component type  
1030000 tank tmdpvol  
\* Volume flow area; volume length; volume volume (calculated if 0);

\* Azimuthal angle; inclination angle; elevation change;  
 \* Wall roughness (1e-9 times hydraulic diameter if 0);  
 \* Hydraulic diameter (calculated if 0); tlpvbf  
 1030101 1.0 1.0 0.0 0.0 90.0 1.0 0.0 0.0 0  
 \* ebt  
 1030200 3  
 \* Search variable (time); P; T  
 1030201 0.0 101.33e3 320.0  
 \*  
 \* Hot leg 2  
 \* Component name; component type  
 1040000 hotleg2 pipe  
 \* Number of elements  
 1040001 6  
 \* Volume flow area; which elements  
 1040101 5.640e-4,6  
 \* Volume length; which elements  
 1040301 0.126620,6  
 \* Volume azimuthal angle; which elements (optional card)  
 1040501 180.0,6  
 \* Volume inclination angle; which elements (required)  
 1040601 0.0,6  
 \* Wall roughness; hydraulic diameter; which elements  
 \* Here for stainless steel: k=0.015mm; copper: k=0.0015mm  
 1040801 1.5e-6,2.680e-2,6  
 \* tlpvbf (see p.113 of Manual Appendix A); which elements  
 1041001 0,6  
 \* jefvcahs (see p.115 of Manual Appendix A); which elements  
 1041101 0,5  
 \* ebt (initial conditions options); P; T; 0; 0; 0; which elements  
 1041201 3,1.01e5,325.0,0.,0.,0.,6  
 \* Junction initial conditions control option  
 \* 0 for velocities, 1 for mass flow rates  
 1041300 1  
 \* Initial liquid velocity; initial gas velocity;  
 \* Interface velocity (enter 0.0); junction number  
 1041301 0.010,0.010,0.,5  
 \*  
 \* Top of HX 1  
 \* Component name; component type  
 2060000 tophx1 pipe  
 \* Number of elements  
 2060001 6  
 \* Volume flow area; which elements  
 2060101 3.333e-4,6  
 \* Volume length; which elements  
 2060301 0.05705,6

\* Volume azimuthal angle; which elements (optional card)  
 2060501 0.0,6  
 \* Volume inclination angle; which elements (required)  
 2060601 -90.0,6  
 \* Wall roughness; hydraulic diameter; which elements  
 \* Here for stainless steel: k=0.015mm; copper: k=0.0015mm  
 2060801 1.5e-6,2.060e-2,6  
 \* tlpvbf (see p.113 of Manual Appendix A); which elements  
 2061001 0,6  
 \* jefvcahs (see p.115 of Manual Appendix A); which elements  
 2061101 0,5  
 \* ebt (initial conditions options); P; T; 0; 0; 0; which elements  
 2061201 3,1.01e5,325.0,0.,0.,0.,6  
 \* Junction initial conditions control option  
 \* 0 for velocities, 1 for mass flow rates  
 2061300 1  
 \* Initial liquid velocity; initial gas velocity;  
 \* Interface velocity (enter 0.0); junction number  
 2061301 0.0025,0.0025,0.,5  
 \*  
 \* Top of HX 2  
 \* Component name; component type  
 2070000 tophx2 pipe  
 \* Number of elements  
 2070001 6  
 \* Volume flow area; which elements  
 2070101 3.333e-4,6  
 \* Volume length; which elements  
 2070301 0.05705,6  
 \* Volume azimuthal angle; which elements (optional card)  
 2070501 0.0,6  
 \* Volume inclination angle; which elements (required)  
 2070601 -90.0,6  
 \* Wall roughness; hydraulic diameter; which elements  
 \* Here for stainless steel: k=0.015mm; copper: k=0.0015mm  
 2070801 1.5e-6,2.060e-2,6  
 \* tlpvbf (see p.113 of Manual Appendix A); which elements  
 2071001 0,6  
 \* jefvcahs (see p.115 of Manual Appendix A); which elements  
 2071101 0,5  
 \* ebt (initial conditions options); P; T; 0; 0; 0; which elements  
 2071201 3,1.01e5,325.0,0.,0.,0.,6

\* Junction initial conditions control option  
 \* 0 for velocities, 1 for mass flow rates  
 2071300 1  
 \* Initial liquid velocity; initial gas velocity;  
 \* Interface velocity (enter 0.0); junction number  
 2071301 0.0025,0.0025,0.,5  
 \*  
 \* Top of HX 3  
 \* Component name; component type  
 2080000 tophx3 pipe  
 \* Number of elements  
 2080001 6  
 \* Volume flow area; which elements  
 2080101 3.333e-4,6  
 \* Volume length; which elements  
 2080301 0.05705,6  
 \* Volume azimuthal angle; which elements  
 (optional card)  
 2080501 0.0,6  
 \* Volume inclination angle; which elements  
 (required)  
 2080601 -90.0,6  
 \* Wall roughness; hydraulic diameter; which  
 elements  
 \* Here for stainless steel: k=0.015mm; copper:  
 k=0.0015mm  
 2080801 1.5e-6,2.060e-2,6  
 \* tlpvbf (see p.113 of Manual Appendix A);  
 which elements  
 2081001 0,6  
 \* jefvcahs (see p.115 of Manual Appendix A);  
 which elements  
 2081101 0,5  
 \* ebt (initial conditions options); P; T; 0; 0; 0;  
 which elements  
 2081201 3,1.01e5,325.0,0.,0.,0.,6  
 \* Junction initial conditions control option  
 \* 0 for velocities, 1 for mass flow rates  
 2081300 1  
 \* Initial liquid velocity; initial gas velocity;  
 \* Interface velocity (enter 0.0); junction number  
 2081301 0.0025,0.0025,0.,5  
 \*  
 \* Top of HX 4  
 \* Component name; component type  
 2090000 tophx4 pipe  
 \* Number of elements  
 2090001 6  
 \* Volume flow area; which elements  
 2090101 3.333e-4,6  
 \* Volume length; which elements  
 2090301 0.05705,6  
 \* Volume azimuthal angle; which elements  
 (optional card)  
 2090501 0.0,6

\* Volume inclination angle; which elements  
 (required)  
 2090601 -90.0,6  
 \* Wall roughness; hydraulic diameter; which  
 elements  
 \* Here for stainless steel: k=0.015mm; copper:  
 k=0.0015mm  
 2090801 1.5e-6,2.060e-2,6  
 \* tlpvbf (see p.113 of Manual Appendix A);  
 which elements  
 2091001 0,6  
 \* jefvcahs (see p.115 of Manual Appendix A);  
 which elements  
 2091101 0,5  
 \* ebt (initial conditions options); P; T; 0; 0; 0;  
 which elements  
 2091201 3,1.01e5,325.0,0.,0.,0.,6  
 \* Junction initial conditions control option  
 \* 0 for velocities, 1 for mass flow rates  
 2091300 1  
 \* Initial liquid velocity; initial gas velocity;  
 \* Interface velocity (enter 0.0); junction number  
 2091301 0.0025,0.0025,0.,5  
 \*  
 \* HX 1  
 \* Component name; component type  
 1060000 hx1 pipe  
 \* Number of elements  
 1060001 60  
 \* Volume flow area; which elements  
 1060101 3.333e-4,60  
 \* Volume length; which elements  
 1060301 0.01685,60  
 \* Volume azimuthal angle; which elements  
 (optional card)  
 1060501 0.0,60  
 \* Volume inclination angle; which elements  
 (required)  
 1060601 -90.0,60  
 \* Wall roughness; hydraulic diameter; which  
 elements  
 \* Here for stainless steel: k=0.015mm  
 1060801 1.5e-6,2.060e-2,60  
 \* tlpvbf (see p.113 of Manual Appendix A);  
 which elements  
 1061001 0,60  
 \* jefvcahs (see p.115 of Manual Appendix A);  
 which elements  
 1061101 0,59  
 \* ebt (initial conditions options); P; T; 0; 0; 0;  
 which elements  
 1061201 3,1.1e5,325.0,0.,0.,0.,60  
 \* Junction initial conditions control option  
 \* 0 for velocities, 1 for mass flow rates  
 1061300 1  
 \* Initial liquid velocity; initial gas velocity;

\* Interface velocity (enter 0.0); junction number  
1061301 0.0025,0.0025,0.,59  
\*  
\* HX 2  
\* Component name; component type  
1070000 hx2 pipe  
\* Number of elements  
1070001 60  
\* Volume flow area; which elements  
1070101 3.333e-4,60  
\* Volume length; which elements  
1070301 0.01685,60  
\* Volume azimuthal angle; which elements  
(optional card)  
1070501 0.0,60  
\* Volume inclination angle; which elements  
(required)  
1070601 -90.0,60  
\* Wall roughness; hydraulic diameter; which  
elements  
\* Here for stainless steel: k=0.015mm  
1070801 1.5e-6,2.060e-2,60  
\* tlpvbf (see p.113 of Manual Appendix A);  
which elements  
1071001 0,60  
\* jefvcahs (see p.115 of Manual Appendix A);  
which elements  
1071101 0,59  
\* ebt (initial conditions options); P; T; 0; 0; 0;  
which elements  
1071201 3,1.1e5,325.0,0.,0.,0.,60  
\* Junction initial conditions control option  
\* 0 for velocities, 1 for mass flow rates  
1071300 1  
\* Initial liquid velocity; initial gas velocity;  
\* Interface velocity (enter 0.0); junction number  
1071301 0.0025,0.0025,0.,59  
\*  
\* HX 3  
\* Component name; component type  
1080000 hx3 pipe  
\* Number of elements  
1080001 60  
\* Volume flow area; which elements  
1080101 3.333e-4,60  
\* Volume length; which elements  
1080301 0.01685,60  
\* Volume azimuthal angle; which elements  
(optional card)  
1080501 0.0,60  
\* Volume inclination angle; which elements  
(required)  
1080601 -90.0,60  
\* Wall roughness; hydraulic diameter; which  
elements  
\* Here for stainless steel: k=0.015mm

1080801 1.5e-6,2.060e-2,60  
\* tlpvbf (see p.113 of Manual Appendix A);  
which elements  
1081001 0,60  
\* jefvcahs (see p.115 of Manual Appendix A);  
which elements  
1081101 0,59  
\* ebt (initial conditions options); P; T; 0; 0; 0;  
which elements  
1081201 3,1.1e5,325.0,0.,0.,0.,60  
\* Junction initial conditions control option  
\* 0 for velocities, 1 for mass flow rates  
1081300 1  
\* Initial liquid velocity; initial gas velocity;  
\* Interface velocity (enter 0.0); junction number  
1081301 0.0025,0.0025,0.,59  
\*  
\* HX 4  
\* Component name; component type  
1090000 hx4 pipe  
\* Number of elements  
1090001 60  
\* Volume flow area; which elements  
1090101 3.333e-4,60  
\* Volume length; which elements  
1090301 0.01685,60  
\* Volume azimuthal angle; which elements  
(optional card)  
1090501 0.0,60  
\* Volume inclination angle; which elements  
(required)  
1090601 -90.0,60  
\* Wall roughness; hydraulic diameter; which  
elements  
\* Here for stainless steel: k=0.015mm  
1090801 1.5e-6,2.060e-2,60  
\* tlpvbf (see p.113 of Manual Appendix A);  
which elements  
1091001 0,60  
\* jefvcahs (see p.115 of Manual Appendix A);  
which elements  
1091101 0,59  
\* ebt (initial conditions options); P; T; 0; 0; 0;  
which elements  
1091201 3,1.1e5,325.0,0.,0.,0.,60  
\* Junction initial conditions control option  
\* 0 for velocities, 1 for mass flow rates  
1091300 1  
\* Initial liquid velocity; initial gas velocity;  
\* Interface velocity (enter 0.0); junction number  
1091301 0.0025,0.0025,0.,59  
\*  
\* Bottom of HX 1  
\* Component name; component type  
3060000 bothx1 pipe  
\* Number of elements

3060001 6  
 \* Volume flow area; which elements  
 3060101 3.333e-4,6  
 \* Volume length; which elements  
 3060301 0.05705,6  
 \* Volume azimuthal angle; which elements  
 (optional card)  
 3060501 0.0,6  
 \* Volume inclination angle; which elements  
 (required)  
 3060601 -90.0,6  
 \* Wall roughness; hydraulic diameter; which  
 elements  
 \* Here for stainless steel: k=0.015mm; copper:  
 k=0.0015mm  
 3060801 1.5e-6,2.060e-2,6  
 \* tlpvbf (see p.113 of Manual Appendix A);  
 which elements  
 3061001 0,6  
 \* jefvcahs (see p.115 of Manual Appendix A);  
 which elements  
 3061101 0,5  
 \* ebt (initial conditions options); P; T; 0; 0; 0;  
 which elements  
 3061201 3,1.01e5,325.0,0.,0.,0.,6  
 \* Junction initial conditions control option  
 \* 0 for velocities, 1 for mass flow rates  
 3061300 1  
 \* Initial liquid velocity; initial gas velocity;  
 \* Interface velocity (enter 0.0); junction number  
 3061301 0.0025,0.0025,0.,5  
 \*  
 \* Bottom of HX 2  
 \* Component name; component type  
 3070000 bothx2 pipe  
 \* Number of elements  
 3070001 6  
 \* Volume flow area; which elements  
 3070101 3.333e-4,6  
 \* Volume length; which elements  
 3070301 0.05705,6  
 \* Volume azimuthal angle; which elements  
 (optional card)  
 3070501 0.0,6  
 \* Volume inclination angle; which elements  
 (required)  
 3070601 -90.0,6  
 \* Wall roughness; hydraulic diameter; which  
 elements  
 \* Here for stainless steel: k=0.015mm; copper:  
 k=0.0015mm  
 3070801 1.5e-6,2.060e-2,6  
 \* tlpvbf (see p.113 of Manual Appendix A);  
 which elements  
 3071001 0,6  
 \* jefvcahs (see p.115 of Manual Appendix A);  
 which elements  
 3071101 0,5  
 \* ebt (initial conditions options); P; T; 0; 0; 0;  
 which elements  
 3071201 3,1.01e5,325.0,0.,0.,0.,6  
 \* Junction initial conditions control option  
 \* 0 for velocities, 1 for mass flow rates  
 3071300 1  
 \* Initial liquid velocity; initial gas velocity;  
 \* Interface velocity (enter 0.0); junction number  
 3071301 0.0025,0.0025,0.,5  
 \*  
 \* Bottom of HX 3  
 \* Component name; component type  
 3080000 bothx3 pipe  
 \* Number of elements  
 3080001 6  
 \* Volume flow area; which elements  
 3080101 3.333e-4,6  
 \* Volume length; which elements  
 3080301 0.05705,6  
 \* Volume azimuthal angle; which elements  
 (optional card)  
 3080501 0.0,6  
 \* Volume inclination angle; which elements  
 (required)  
 3080601 -90.0,6  
 \* Wall roughness; hydraulic diameter; which  
 elements  
 \* Here for stainless steel: k=0.015mm; copper:  
 k=0.0015mm  
 3080801 1.5e-6,2.060e-2,6  
 \* tlpvbf (see p.113 of Manual Appendix A);  
 which elements  
 3081001 0,6  
 \* jefvcahs (see p.115 of Manual Appendix A);  
 which elements  
 3081101 0,5  
 \* ebt (initial conditions options); P; T; 0; 0; 0;  
 which elements  
 3081201 3,1.01e5,325.0,0.,0.,0.,6  
 \* Junction initial conditions control option  
 \* 0 for velocities, 1 for mass flow rates  
 3081300 1  
 \* Initial liquid velocity; initial gas velocity;  
 \* Interface velocity (enter 0.0); junction number  
 3081301 0.0025,0.0025,0.,5  
 \*  
 \* Bottom of HX 4  
 \* Component name; component type  
 3090000 bothx4 pipe  
 \* Number of elements  
 3090001 6  
 \* Volume flow area; which elements  
 3090101 3.333e-4,6

\* Volume length; which elements  
3090301 0.05705,6

\* Volume azimuthal angle; which elements  
(optional card)  
3090501 0.0,6

\* Volume inclination angle; which elements  
(required)  
3090601 -90.0,6

\* Wall roughness; hydraulic diameter; which elements  
\* Here for stainless steel:  $k=0.015\text{mm}$ ; copper:  
 $k=0.0015\text{mm}$   
3090801  $1.5\text{e-}6,2.060\text{e-}2,6$

\* tlpvbf (see p.113 of Manual Appendix A);  
which elements  
3091001 0,6

\* jefvcahs (see p.115 of Manual Appendix A);  
which elements  
3091101 0,5

\* ebt (initial conditions options); P; T; 0; 0; 0;  
which elements  
3091201  $3,1.01\text{e}5,325.0,0.,0.,0.,6$

\* Junction initial conditions control option  
\* 0 for velocities, 1 for mass flow rates  
3091300 1

\* Initial liquid velocity; initial gas velocity;  
\* Interface velocity (enter 0.0); junction number  
3091301  $0.0025,0.0025,0.,5$

\*

\* Cold leg

\* Component name; component type  
1110000 coldleg pipe

\* Number of elements  
1110001 16

\* Volume flow area; which elements  
1110101  $5.640\text{e-}4,12$   
1110102  $9.9074\text{e-}5,16$

\* Volume length; which elements  
1110301  $9.5940\text{e-}2,6$   
1110302  $0.12662,12$   
1110303  $4.00625\text{e-}2,16$

\* Volume azimuthal angle; which elements  
(optional card)  
1110501 0.0,16

\* Volume inclination angle; which elements  
(required)  
1110601 -90.0,6  
1110602 0.0,12  
1110603 90.0,16

\* Wall roughness; hydraulic diameter; which elements  
\* Here for stainless steel:  $k=0.015\text{mm}$ ; copper:  
 $k=0.0015\text{mm}$   
1110801  $1.5\text{e-}6,2.680\text{e-}2,12$   
1110802  $1.5\text{e-}5,3.860\text{e-}3,16$

\* tlpvbf (see p.113 of Manual Appendix A);  
which elements  
1111001 0,16

\* jefvcahs (see p.115 of Manual Appendix A);  
which elements  
1111101 0,11  
1111102 100,12 \* Abrupt area change  
1111103 0,15

\* ebt (initial conditions options); P; T; 0.; 0.; 0.;  
which elements  
1111201  $3,1.5\text{e}5,325.0,0.,0.,0.,16$

\* Junction initial conditions control option  
\* 0 for velocities, 1 for mass flow rates  
1111300 1

\* Initial liquid velocity; initial gas velocity;  
\* Interface velocity (enter 0.0); junction number  
1111301  $0.010,0.010,0.,15$

\*

\* Junction 100-101

\* Component name; component type  
4000000 jn100101 sngljun

\* From; to; junction area; A\_f; A\_r; jefvcahs  
4000101 100010000 101000000  $9.9074\text{e-}5$  0. 0.  
0

\* Control word (0 for velocities, 1 for mass flow rates)  
\* Initial liquid velocity; initial gas velocity;  
\* Interface velocity (enter 0.0)  
4000201 1 0.010 0.010 0.

\*

\* Junction 206-106

\* Component name; component type  
4060000 jn206106 sngljun

\* From; to; junction area; A\_f; A\_r; jefvcahs  
4060101 206010000 106000000  $3.333\text{e-}4$  0. 0. 0

\* Control word (0 for velocities, 1 for mass flow rates)  
\* Initial liquid velocity; initial gas velocity;  
\* Interface velocity (enter 0.0)  
4060201 1 0.0025 0.0025 0.

\*

\* Junction 207-107

\* Component name; component type  
4070000 jn207107 sngljun

\* From; to; junction area; A\_f; A\_r; jefvcahs  
4070101 207010000 107000000  $3.333\text{e-}4$  0. 0. 0

\* Control word (0 for velocities, 1 for mass flow rates)  
\* Initial liquid velocity; initial gas velocity;  
\* Interface velocity (enter 0.0)  
4070201 1 0.0025 0.0025 0.

\*

\* Junction 208-108

\* Component name; component type  
4080000 jn208108 sngljun

\* From; to; junction area; A\_f; A\_r; jefvcahs

4080101 208010000 108000000 3.333e-4 0. 0. 0  
 \* Control word (0 for velocities, 1 for mass flow rates)  
 \* Initial liquid velocity; initial gas velocity;  
 \* Interface velocity (enter 0.0)  
 4080201 1 0.0025 0.0025 0.  
 \*  
 \* Junction 209-109  
 \* Component name; component type  
 4090000 jn209109 sngljun  
 \* From; to; junction area; A\_f; A\_r; jefvcahs  
 4090101 209010000 109000000 3.333e-4 0. 0. 0  
 \* Control word (0 for velocities, 1 for mass flow rates)  
 \* Initial liquid velocity; initial gas velocity;  
 \* Interface velocity (enter 0.0)  
 4090201 1 0.0025 0.0025 0.  
 \*  
 \* Junction 106-306  
 \* Component name; component type  
 4160000 jn106306 sngljun  
 \* From; to; junction area; A\_f; A\_r; jefvcahs  
 4160101 106010000 306000000 3.333e-4 0. 0. 0  
 \* Control word (0 for velocities, 1 for mass flow rates)  
 \* Initial liquid velocity; initial gas velocity;  
 \* Interface velocity (enter 0.0)  
 4160201 1 0.0025 0.0025 0.  
 \*  
 \* Junction 107-307  
 \* Component name; component type  
 4170000 jn107307 sngljun  
 \* From; to; junction area; A\_f; A\_r; jefvcahs  
 4170101 107010000 307000000 3.333e-4 0. 0. 0  
 \* Control word (0 for velocities, 1 for mass flow rates)  
 \* Initial liquid velocity; initial gas velocity;  
 \* Interface velocity (enter 0.0)  
 4170201 1 0.0025 0.0025 0.  
 \*  
 \* Junction 108-308  
 \* Component name; component type  
 4180000 jn108308 sngljun  
 \* From; to; junction area; A\_f; A\_r; jefvcahs  
 4180101 108010000 308000000 3.333e-4 0. 0. 0  
 \* Control word (0 for velocities, 1 for mass flow rates)  
 \* Initial liquid velocity; initial gas velocity;  
 \* Interface velocity (enter 0.0)  
 4180201 1 0.0025 0.0025 0.  
 \*  
 \* Junction 109-309  
 \* Component name; component type  
 4190000 jn109309 sngljun  
 \* From; to; junction area; A\_f; A\_r; jefvcahs  
 4190101 109010000 309000000 3.333e-4 0. 0. 0

\* Control word (0 for velocities, 1 for mass flow rates)  
 \* Initial liquid velocity; initial gas velocity;  
 \* Interface velocity (enter 0.0)  
 4190201 1 0.0025 0.0025 0.  
 \*  
 \* Junction 111-100  
 \* Component name; component type  
 4110000 jn111100 sngljun  
 \* From; to; junction area; A\_f; A\_r; jefvcahs  
 4110101 111010000 100000000 9.9074e-5 0. 0. 0  
 \* Control word (0 for velocities, 1 for mass flow rates)  
 \* Initial liquid velocity; initial gas velocity;  
 \* Interface velocity (enter 0.0)  
 4110201 1 0.010 0.010 0.  
 \*  
 \* Branch 102  
 \* Component name; component type  
 1020000 br102 branch  
 \* Number of junctions; control word (0: velocities, 1: mass flow rates)  
 1020001 3 1  
 \* Volume flow area; volume length; volume of volume (calculated if 0.0)  
 \* Azimuthal angle; vertical angle; elevation change; wall roughness  
 \* Hydraulic diameter; tlpvbf  
 1020101 5.640e-4 0.02680 0. 0. 90. 0.02680  
 1.5e-6 0.02680 0  
 \* ebt (initial conditions options); P; T  
 1020200 3 1.1e5 325.0  
 \* From; to; junction area; A\_f; A\_r; jefvcahs  
 1021101 101010000 102000000 5.640e-4 0. 0. 0  
 1022101 102010000 103000000 5.640e-4 0. 0. 100  
 1023101 102010000 104000000 5.640e-4 0. 0. 0  
 \* Initial liquid velocity; initial gas velocity;  
 \* Interface velocity (enter 0.0)  
 1021201 0.010 0.010 0.  
 1022201 0.000 0.000 0.  
 1023201 0.010 0.010 0.  
 \*  
 \* Branch 105  
 \* Component name; component type  
 1050000 br105 branch  
 \* Number of junctions; control word (0: velocities, 1: mass flow rates)  
 1050001 5 1  
 \* Volume flow area; volume length; volume of volume (calculated if 0.0)  
 \* Azimuthal angle; vertical angle; elevation change; wall roughness  
 \* Hydraulic diameter; tlpvbf

1050101 5.640e-4 0.53155 0. 0. -90. -0.53155  
1.5e-6 0.02680 0  
\* ebt (initial conditions options); P; T  
1050200 3 1.1e5 325.0  
\* From; to; junction area; A\_f; A\_r; jefvcahs  
1051101 104010000 105000000 5.640e-4 0. 0. 0  
1052101 105010000 206000000 3.333e-4 0. 0. 0  
1053101 105010000 207000000 3.333e-4 0. 0. 0  
1054101 105010000 208000000 3.333e-4 0. 0. 0  
1055101 105010000 209000000 3.333e-4 0. 0. 0  
\* Initial liquid velocity; initial gas velocity;  
\* Interface velocity (enter 0.0)  
1051201 0.010 0.010 0.  
1052201 0.0025 0.0025 0.  
1053201 0.0025 0.0025 0.  
1054201 0.0025 0.0025 0.  
1055201 0.0025 0.0025 0.  
\*  
\* Branch 110  
\* Component name; component type  
1100000 br110 branch  
\* Number of junctions; control word (0:  
velocities, 1: mass flow rates)  
1100001 5 1  
\* Volume flow area; volume length; volume of  
volume (calculated if 0.0)  
\* Azimuthal angle; vertical angle; elevation  
change; wall roughness  
\* Hydraulic diameter; tlpvbf  
1100101 5.640e-4 0.53155 0. 0. -90. -0.53155  
1.5e-6 0.02680 0  
\* ebt (initial conditions options); P; T  
1100200 3 1.5e5 325.0  
\* From; to; junction area; A\_f; A\_r; jefvcahs  
1101101 306010000 110000000 3.333e-4 0. 0. 0  
1102101 307010000 110000000 3.333e-4 0. 0. 0  
1103101 308010000 110000000 3.333e-4 0. 0. 0  
1104101 309010000 110000000 3.333e-4 0. 0. 0  
1105101 110010000 111000000 5.640e-4 0. 0. 0  
\* Initial liquid velocity; initial gas velocity;  
\* Interface velocity (enter 0.0)  
1101201 0.0025 0.0025 0.  
1102201 0.0025 0.0025 0.  
1103201 0.0025 0.0025 0.  
1104201 0.0025 0.0025 0.  
1105201 0.010 0.010 0.  
\*  
\*\*\*\*\*  
\* Heat structures  
\*\*\*\*\*  
\*  
\* Heater outer tube  
\* Number of axial heat structures; number of  
radial mesh points;  
\* Geometry type (2: cylindrical, coupled to  
hydrodynamic component);

\* Steady-state initialization flag (1: initial T  
calculated by code);  
\* Left boundary coordinate; reflow condition  
11001000 60 3 2 1 0.009135 0  
\* Mesh location flag; mesh format flag (see  
p.207 of Manual Appendix A)  
11001100 0 1  
\* Number of intervals; right coordinate  
11001101 1 0.0127  
11001102 1 0.0889  
\* Composition (table number); interval number  
11001201 100 1  
11001202 120 2  
\* Power input proportion; mesh interval number  
11001301 1.0 1  
11001302 0.0 2  
\* Initial temperature flag (see p.208 of Manual  
Appendix A)  
11001400 0  
\* Initial temperature; mesh point number  
11001401 325.0 2  
11001402 293.15 3  
\* Left boundary condition definition (here: vol  
number); increment;  
\* Boundary condition type (101: convection);  
surface area code (1: length);  
\* Length; heat structure number  
11001501 100010000 10000 101 1 0.024342 60  
\* Right boundary condition, see above (-30: T  
defined in general table 30; 1000: T set in Word  
1)  
11001601 -30 0 1000 1 0.024342 60  
\* Power source (table number); internal source  
multiplier; direct mod heatin mult (left)  
\* Direct mod heatin mult (right); heat structure  
number  
11001701 10 0.016666667 0.0 0.0 60  
\* Additional left boundary: heat transfer  
hydraulic diameter; heated length fwd (10.:  
ignore);  
\* Heated length rev (10.: ignore); grid spacer  
length fwd (0.: ignore); grid spacer length rev  
(0.: ignore);  
\* Grid loss coef fwd (0.: ignore); grid loss coef  
rev (0.: ignore); boiling factor (1.: subcooled  
liquid);  
\* Heat structure number  
11001801 0.006904 10.0 10.0 0.0 0.0 0.0 1.0  
60  
\*  
\* Heater inner tube  
\* Number of axial heat structures; number of  
radial mesh points;  
\* Geometry type (2: cylindrical, coupled to  
hydrodynamic component);

\* Steady-state initialization flag (1: initial T calculated by code);  
 \* Left boundary coordinate (schedule 40 stainless steel); reflow condition  
 11002000 60 2 2 1 0.004623 0  
 \* Mesh location flag; mesh format flag (see p.207 of Manual Appendix A)  
 11002100 0 1  
 \* Number of intervals; right coordinate  
 11002101 1 0.007205  
 \* Composition (table number); interval number  
 11002201 100 1  
 \* Power input proportion; mesh interval number  
 11002301 1.0 1  
 \* Initial temperature flag (see p.208 of Manual Appendix A)  
 11002400 0  
 \* Initial temperature; mesh point number  
 11002401 325.0 2  
 \* Left boundary condition definition (0: adiabatic); increment;  
 \* Boundary condition type (0: adiabatic); surface area code (1: length);  
 \* Length; heat structure number  
 11002501 0 0 0 1 0.024342 60  
 \* Right boundary condition, see above (101: convection)  
 11002601 100010000 10000 101 1 0.024342 60  
 \* Power source (no source); internal source multiplier; direct mod heatin mult (left)  
 \* Direct mod heatin mult (right); heat structure number  
 11002701 0 0.0 0.0 0.0 60  
 \* Additional right boundary: heat transfer hydraulic diameter; heated length fwd (10.: ignore);  
 \* Heated length rev (10.: ignore); grid spacer length fwd (0.: ignore); grid spacer length rev (0.: ignore);  
 \* Grid loss coef fwd (0.: ignore); grid loss coef rev (0.: ignore); boiling factor (1.: subcooled liquid);  
 \* Heat structure number  
 11002901 0.008754 10.0 10.0 0.0 0.0 0.0 1.0 60  
 \*  
 \* HX1  
 \* Number of axial heat structures; number of radial mesh points;  
 \* Geometry type (2: cylindrical, coupled to hydrodynamic component);  
 \* Steady-state initialization flag (1: initial T calculated by code);  
 \* Left boundary coordinate; reflow condition  
 11061000 60 2 2 1 0.0102997 0

\* Mesh location flag; mesh format flag (see p.207 of Manual Appendix A)  
 11061100 0 1  
 \* Number of intervals; right coordinate  
 11061101 1 0.0111125  
 \* Composition (table number); interval number  
 11061201 110 1  
 \* Power input proportion; mesh interval number  
 11061301 1.0 1  
 \* Initial temperature flag (see p.208 of Manual Appendix A)  
 11061400 0  
 \* Initial temperature; mesh point number  
 11061401 325.0 2  
 \* Left boundary condition definition (here: vol number); increment;  
 \* Boundary condition type (101: convection); surface area code (1: length);  
 \* Length; heat structure number  
 11061501 106010000 10000 101 1 0.01685 60  
 \* Right boundary condition, see above (-20: T defined in general table 20; 1000: T set in Word 1)  
 11061601 -20 0 1000 1 0.01685 60  
 \* Power source (no source); internal source multiplier; direct mod heatin mult (left)  
 \* Direct mod heatin mult (right); heat structure number  
 11061701 0 0.0 0.0 0.0 60  
 \* Additional left boundary: heat transfer hydraulic diameter; heated length fwd (10.: ignore);  
 \* Heated length rev (10.: ignore); grid spacer length fwd (0.: ignore); grid spacer length rev (0.: ignore);  
 \* Grid loss coef fwd (0.: ignore); grid loss coef rev (0.: ignore); boiling factor (1.: subcooled liquid);  
 \* Heat structure number  
 11061801 0.0 10.0 10.0 0.0 0.0 0.0 1.0 60  
 \*  
 \* HX2  
 \* Number of axial heat structures; number of radial mesh points;  
 \* Geometry type (2: cylindrical, coupled to hydrodynamic component);  
 \* Steady-state initialization flag (1: initial T calculated by code);  
 \* Left boundary coordinate; reflow condition  
 11071000 60 2 2 1 0.0102997 0  
 \* Mesh location flag; mesh format flag (see p.207 of Manual Appendix A)  
 11071100 0 1  
 \* Number of intervals; right coordinate  
 11071101 1 0.0111125  
 \* Composition (table number); interval number

11071201 110 1  
 \* Power input proportion; mesh interval number  
 11071301 1.0 1  
 \* Initial temperature flag (see p.208 of Manual Appendix A)  
 11071400 0  
 \* Initial temperature; mesh point number  
 11071401 325.0 2  
 \* Left boundary condition definition (here: vol number); increment;  
 \* Boundary condition type (101: convection); surface area code (1: length);  
 \* Length; heat structure number  
 11071501 107010000 10000 101 1 0.01685 60  
 \* Right boundary condition, see above (-20: T defined in general table 20; 1000: T set in Word 1)  
 11071601 -20 0 1000 1 0.01685 60  
 \* Power source (no source); internal source multiplier; direct mod heatin mult (left)  
 \* Direct mod heatin mult (right); heat structure number  
 11071701 0 0.0 0.0 0.0 60  
 \* Additional left boundary: heat transfer hydraulic diameter; heated length fwd (10.: ignore);  
 \* Heated length rev (10.: ignore); grid spacer length fwd (0.: ignore); grid spacer length rev (0.: ignore);  
 \* Grid loss coef fwd (0.: ignore); grid loss coef rev (0.: ignore); boiling factor (1.: subcooled liquid);  
 \* Heat structure number  
 11071801 0.0 10.0 10.0 0.0 0.0 0.0 1.0 60  
 \*  
 \* HX3  
 \* Number of axial heat structures; number of radial mesh points;  
 \* Geometry type (2: cylindrical, coupled to hydrodynamic component);  
 \* Steady-state initialization flag (1: initial T calculated by code);  
 \* Left boundary coordinate; reflow condition  
 11081000 60 2 2 1 0.0102997 0  
 \* Mesh location flag; mesh format flag (see p.207 of Manual Appendix A)  
 11081100 0 1  
 \* Number of intervals; right coordinate  
 11081101 1 0.0111125  
 \* Composition (table number); interval number  
 11081201 110 1  
 \* Power input proportion; mesh interval number  
 11081301 1.0 1  
 \* Initial temperature flag (see p.208 of Manual Appendix A)  
 11081400 0

\* Initial temperature; mesh point number  
 11081401 325.0 2  
 \* Left boundary condition definition (here: vol number); increment;  
 \* Boundary condition type (101: convection); surface area code (1: length);  
 \* Length; heat structure number  
 11081501 108010000 10000 101 1 0.01685 60  
 \* Right boundary condition, see above (-20: T defined in general table 20; 1000: T set in Word 1)  
 11081601 -20 0 1000 1 0.01685 60  
 \* Power source (no source); internal source multiplier; direct mod heatin mult (left)  
 \* Direct mod heatin mult (right); heat structure number  
 11081701 0 0.0 0.0 0.0 60  
 \* Additional left boundary: heat transfer hydraulic diameter; heated length fwd (10.: ignore);  
 \* Heated length rev (10.: ignore); grid spacer length fwd (0.: ignore); grid spacer length rev (0.: ignore);  
 \* Grid loss coef fwd (0.: ignore); grid loss coef rev (0.: ignore); boiling factor (1.: subcooled liquid);  
 \* Heat structure number  
 11081801 0.0 10.0 10.0 0.0 0.0 0.0 1.0 60  
 \*  
 \* HX4  
 \* Number of axial heat structures; number of radial mesh points;  
 \* Geometry type (2: cylindrical, coupled to hydrodynamic component);  
 \* Steady-state initialization flag (1: initial T calculated by code);  
 \* Left boundary coordinate; reflow condition  
 11091000 60 2 2 1 0.0102997 0  
 \* Mesh location flag; mesh format flag (see p.207 of Manual Appendix A)  
 11091100 0 1  
 \* Number of intervals; right coordinate  
 11091101 1 0.0111125  
 \* Composition (table number); interval number  
 11091201 110 1  
 \* Power input proportion; mesh interval number  
 11091301 1.0 1  
 \* Initial temperature flag (see p.208 of Manual Appendix A)  
 11091400 0  
 \* Initial temperature; mesh point number  
 11091401 325.0 2  
 \* Left boundary condition definition (here: vol number); increment;  
 \* Boundary condition type (101: convection); surface area code (1: length);

\* Length; heat structure number  
11091501 109010000 10000 101 1 0.01685 60  
\* Right boundary condition, see above (-20: T defined in general table 20; 1000: T set in Word 1)  
11091601 -20 0 1000 1 0.01685 60  
\* Power source (no source); internal source multiplier; direct mod heatin mult (left)  
\* Direct mod heatin mult (right); heat structure number  
11091701 0 0.0 0.0 0.0 60  
\* Additional left boundary: heat transfer hydraulic diameter; heated length fwd (10.: ignore);  
\* Heated length rev (10.: ignore); grid spacer length fwd (0.: ignore); grid spacer length rev (0.: ignore);  
\* Grid loss coef fwd (0.: ignore); grid loss coef rev (0.: ignore); boiling factor (1.: subcooled liquid);  
\* Heat structure number  
11091801 0.0 10.0 10.0 0.0 0.0 0.0 1.0 60  
\*  
\* Top of heater outer tube  
\* Number of axial heat structures; number of radial mesh points;  
\* Geometry type (2: cylindrical, coupled to hydrodynamic component);  
\* Steady-state initialization flag (1: initial T calculated by code);  
\* Left boundary coordinate; reflood condition  
11011000 4 3 2 1 0.009135 0  
\* Mesh location flag; mesh format flag (see p.207 of Manual Appendix A)  
11011100 0 1  
\* Number of intervals; right coordinate  
11011101 1 0.0127  
11011102 1 0.0889  
\* Composition (table number); interval number  
11011201 100 1  
11011202 120 2  
\* Power input proportion; mesh interval number  
11011301 1.0 1  
11011302 0.0 2  
\* Initial temperature flag (see p.208 of Manual Appendix A)  
11011400 0  
\* Initial temperature; mesh point number  
11011401 325.0 2  
11011402 293.15 3  
\* Left boundary condition definition (here: vol number); increment;  
\* Boundary condition type (101: convection); surface area code (1: length);  
\* Length; heat structure number  
11011501 101010000 10000 101 1 0.0400625 4

\* Right boundary condition, see above (-30: T defined in general table 30; 1000: T set in Word 1)  
11011601 -30 0 1000 1 0.0400625 4  
\* Power source (table number); internal source multiplier; direct mod heatin mult (left)  
\* Direct mod heatin mult (right); heat structure number  
11011701 0 0.0 0.0 0.0 4  
\* Additional left boundary: heat transfer hydraulic diameter; heated length fwd (10.: ignore);  
\* Heated length rev (10.: ignore); grid spacer length fwd (0.: ignore); grid spacer length rev (0.: ignore);  
\* Grid loss coef fwd (0.: ignore); grid loss coef rev (0.: ignore); boiling factor (1.: subcooled liquid);  
\* Heat structure number  
11011801 0.006904 10.0 10.0 0.0 0.0 0.0 1.0 4  
\*  
\* Top of heater inner tube  
\* Number of axial heat structures; number of radial mesh points;  
\* Geometry type (2: cylindrical, coupled to hydrodynamic component);  
\* Steady-state initialization flag (1: initial T calculated by code);  
\* Left boundary coordinate (schedule 40 stainless steel); reflood condition  
11012000 4 2 2 1 0.004623 0  
\* Mesh location flag; mesh format flag (see p.207 of Manual Appendix A)  
11012100 0 1  
\* Number of intervals; right coordinate  
11012101 1 0.007205  
\* Composition (table number); interval number  
11012201 100 1  
\* Power input proportion; mesh interval number  
11012301 1.0 1  
\* Initial temperature flag (see p.208 of Manual Appendix A)  
11012400 0  
\* Initial temperature; mesh point number  
11012401 325.0 2  
\* Left boundary condition definition (0: adiabatic); increment;  
\* Boundary condition type (0: adiabatic); surface area code (1: length);  
\* Length; heat structure number  
11012501 0 0 0 1 0.0400625 4  
\* Right boundary condition, see above (101: convection)  
11012601 101010000 10000 101 1 0.0400625 4

\* Power source (no source); internal source multiplier; direct mod heatin mult (left)  
 \* Direct mod heatin mult (right); heat structure number  
 11012701 0 0.0 0.0 0.0 4  
 \* Additional right boundary: heat transfer hydraulic diameter; heated length fwd (10.: ignore);  
 \* Heated length rev (10.: ignore); grid spacer length fwd (0.: ignore); grid spacer length rev (0.: ignore);  
 \* Grid loss coef fwd (0.: ignore); grid loss coef rev (0.: ignore); boiling factor (1.: subcooled liquid);  
 \* Heat structure number  
 11012901 0.008754 10.0 10.0 0.0 0.0 0.0 1.0 4  
 \*  
 \* Hot leg 1  
 \* Number of axial heat structures; number of radial mesh points;  
 \* Geometry type (2: cylindrical, coupled to hydrodynamic component);  
 \* Steady-state initialization flag (1: initial T calculated by code);  
 \* Left boundary coordinate; reflood condition  
 11013000 12 3 2 1 0.0133985 0  
 \* Mesh location flag; mesh format flag (see p.207 of Manual Appendix A)  
 11013100 0 1  
 \* Number of intervals; right coordinate  
 11013101 1 0.0142875  
 11013102 1 0.0904875  
 \* Composition (table number); interval number  
 11013201 110 1  
 11013202 120 2  
 \* Power input proportion; mesh interval number  
 11013301 1.0 1  
 11013302 0.0 2  
 \* Initial temperature flag (see p.208 of Manual Appendix A)  
 11013400 0  
 \* Initial temperature; mesh point number  
 11013401 325.0 2  
 11013402 293.15 3  
 \* Left boundary condition definition (here: vol number); increment;  
 \* Boundary condition type (101: convection); surface area code (1: length);  
 \* Length; heat structure number  
 11013501 101050000 10000 101 1 0.12721 12  
 \* Right boundary condition, see above (-30: T defined in general table 30; 1000: T set in Word 1)  
 11013601 -30 0 1000 1 0.12721 12

\* Power source (table number); internal source multiplier; direct mod heatin mult (left)  
 \* Direct mod heatin mult (right); heat structure number  
 11013701 0 0.0 0.0 0.0 12  
 \* Additional left boundary: heat transfer hydraulic diameter; heated length fwd (10.: ignore);  
 \* Heated length rev (10.: ignore); grid spacer length fwd (0.: ignore); grid spacer length rev (0.: ignore);  
 \* Grid loss coef fwd (0.: ignore); grid loss coef rev (0.: ignore); boiling factor (1.: subcooled liquid);  
 \* Heat structure number  
 11013801 0.0 10.0 10.0 0.0 0.0 0.0 1.0 12  
 \*  
 \* Hot leg 2  
 \* Number of axial heat structures; number of radial mesh points;  
 \* Geometry type (2: cylindrical, coupled to hydrodynamic component);  
 \* Steady-state initialization flag (1: initial T calculated by code);  
 \* Left boundary coordinate; reflood condition  
 11021000 1 3 2 1 0.0133985 0  
 \* Mesh location flag; mesh format flag (see p.207 of Manual Appendix A)  
 11021100 0 1  
 \* Number of intervals; right coordinate  
 11021101 1 0.0142875  
 11021102 1 0.0904875  
 \* Composition (table number); interval number  
 11021201 110 1  
 11021202 120 2  
 \* Power input proportion; mesh interval number  
 11021301 1.0 1  
 11021302 0.0 2  
 \* Initial temperature flag (see p.208 of Manual Appendix A)  
 11021400 0  
 \* Initial temperature; mesh point number  
 11021401 325.0 2  
 11021402 293.15 3  
 \* Left boundary condition definition (here: vol number); increment;  
 \* Boundary condition type (101: convection); surface area code (1: length);  
 \* Length; heat structure number  
 11021501 102010000 10000 101 1 0.02680 1  
 \* Right boundary condition, see above (-30: T defined in general table 30; 1000: T set in Word 1)  
 11021601 -30 0 1000 1 0.02680 1  
 \* Power source (table number); internal source multiplier; direct mod heatin mult (left)

\* Direct mod heatin mult (right); heat structure number  
11021701 0 0.0 0.0 0.0 1  
\* Additional left boundary: heat transfer hydraulic diameter; heated length fwd (10.: ignore);  
\* Heated length rev (10.: ignore); grid spacer length fwd (0.: ignore); grid spacer length rev (0.: ignore);  
\* Grid loss coef fwd (0.: ignore); grid loss coef rev (0.: ignore); boiling factor (1.: subcooled liquid);  
\* Heat structure number  
11021801 0.0 10.0 10.0 0.0 0.0 0.0 1.0 1  
\*  
\* Hot leg 3  
\* Number of axial heat structures; number of radial mesh points;  
\* Geometry type (2: cylindrical, coupled to hydrodynamic component);  
\* Steady-state initialization flag (1: initial T calculated by code);  
\* Left boundary coordinate; reflow condition  
11041000 6 3 2 1 0.0133985 0  
\* Mesh location flag; mesh format flag (see p.207 of Manual Appendix A)  
11041100 0 1  
\* Number of intervals; right coordinate  
11041101 1 0.0142875  
11041102 1 0.0904875  
\* Composition (table number); interval number  
11041201 110 1  
11041202 120 2  
\* Power input proportion; mesh interval number  
11041301 1.0 1  
11041302 0.0 2  
\* Initial temperature flag (see p.208 of Manual Appendix A)  
11041400 0  
\* Initial temperature; mesh point number  
11041401 325.0 2  
11041402 293.15 3  
\* Left boundary condition definition (here: vol number); increment;  
\* Boundary condition type (101: convection); surface area code (1: length);  
\* Length; heat structure number  
11041501 104010000 10000 101 1 0.126620 6  
\* Right boundary condition, see above (-30: T defined in general table 30; 1000: T set in Word 1)  
11041601 -30 0 1000 1 0.126620 6  
\* Power source (table number); internal source multiplier; direct mod heatin mult (left)  
\* Direct mod heatin mult (right); heat structure number

11041701 0 0.0 0.0 0.0 6  
\* Additional left boundary: heat transfer hydraulic diameter; heated length fwd (10.: ignore);  
\* Heated length rev (10.: ignore); grid spacer length fwd (0.: ignore); grid spacer length rev (0.: ignore);  
\* Grid loss coef fwd (0.: ignore); grid loss coef rev (0.: ignore); boiling factor (1.: subcooled liquid);  
\* Heat structure number  
11041801 0.0 10.0 10.0 0.0 0.0 0.0 1.0 6  
\*  
\* Hot leg 4  
\* Number of axial heat structures; number of radial mesh points;  
\* Geometry type (2: cylindrical, coupled to hydrodynamic component);  
\* Steady-state initialization flag (1: initial T calculated by code);  
\* Left boundary coordinate; reflow condition  
11051000 1 3 2 1 0.0133985 0  
\* Mesh location flag; mesh format flag (see p.207 of Manual Appendix A)  
11051100 0 1  
\* Number of intervals; right coordinate  
11051101 1 0.0142875  
11051102 1 0.0904875  
\* Composition (table number); interval number  
11051201 110 1  
11051202 120 2  
\* Power input proportion; mesh interval number  
11051301 1.0 1  
11051302 0.0 2  
\* Initial temperature flag (see p.208 of Manual Appendix A)  
11051400 0  
\* Initial temperature; mesh point number  
11051401 325.0 2  
11051402 293.15 3  
\* Left boundary condition definition (here: vol number); increment;  
\* Boundary condition type (101: convection); surface area code (1: length);  
\* Length; heat structure number  
11051501 105010000 10000 101 1 0.53155 1  
\* Right boundary condition, see above (-30: T defined in general table 30; 1000: T set in Word 1)  
11051601 -30 0 1000 1 0.53155 1  
\* Power source (table number); internal source multiplier; direct mod heatin mult (left)  
\* Direct mod heatin mult (right); heat structure number  
11051701 0 0.0 0.0 0.0 1

\* Additional left boundary: heat transfer hydraulic diameter; heated length fwd (10.: ignore);  
 \* Heated length rev (10.: ignore); grid spacer length fwd (0.: ignore); grid spacer length rev (0.: ignore);  
 \* Grid loss coef fwd (0.: ignore); grid loss coef rev (0.: ignore); boiling factor (1.: subcooled liquid);  
 \* Heat structure number  
 11051801 0.0 10.0 10.0 0.0 0.0 0.0 0.0 1.0 1  
 \*  
 \* Cold leg 1  
 \* Number of axial heat structures; number of radial mesh points;  
 \* Geometry type (2: cylindrical, coupled to hydrodynamic component);  
 \* Steady-state initialization flag (1: initial T calculated by code);  
 \* Left boundary coordinate; reflow condition  
 11101000 1 3 2 1 0.0133985 0  
 \* Mesh location flag; mesh format flag (see p.207 of Manual Appendix A)  
 11101100 0 1  
 \* Number of intervals; right coordinate  
 11101101 1 0.0142875  
 11101102 1 0.0904875  
 \* Composition (table number); interval number  
 11101201 110 1  
 11101202 120 2  
 \* Power input proportion; mesh interval number  
 11101301 1.0 1  
 11101302 0.0 2  
 \* Initial temperature flag (see p.208 of Manual Appendix A)  
 11101400 0  
 \* Initial temperature; mesh point number  
 11101401 325.0 2  
 11101402 293.15 3  
 \* Left boundary condition definition (here: vol number); increment;  
 \* Boundary condition type (101: convection); surface area code (1: length);  
 \* Length; heat structure number  
 11101501 111010000 10000 101 1 0.53155 1  
 \* Right boundary condition, see above (-30: T defined in general table 30; 1000: T set in Word 1)  
 11101601 -30 0 1000 1 0.53155 1  
 \* Power source (table number); internal source multiplier; direct mod heatin mult (left)  
 \* Direct mod heatin mult (right); heat structure number  
 11101701 0 0.0 0.0 0.0 1

\* Additional left boundary: heat transfer hydraulic diameter; heated length fwd (10.: ignore);  
 \* Heated length rev (10.: ignore); grid spacer length fwd (0.: ignore); grid spacer length rev (0.: ignore);  
 \* Grid loss coef fwd (0.: ignore); grid loss coef rev (0.: ignore); boiling factor (1.: subcooled liquid);  
 \* Heat structure number  
 11101801 0.0 10.0 10.0 0.0 0.0 0.0 0.0 1.0 1  
 \*  
 \* Cold leg 2  
 \* Number of axial heat structures; number of radial mesh points;  
 \* Geometry type (2: cylindrical, coupled to hydrodynamic component);  
 \* Steady-state initialization flag (1: initial T calculated by code);  
 \* Left boundary coordinate; reflow condition  
 11111000 12 3 2 1 0.0133985 0  
 \* Mesh location flag; mesh format flag (see p.207 of Manual Appendix A)  
 11111100 0 1  
 \* Number of intervals; right coordinate  
 11111101 1 0.0142875  
 11111102 1 0.0904875  
 \* Composition (table number); interval number  
 11111201 110 1  
 11111202 120 2  
 \* Power input proportion; mesh interval number  
 11111301 1.0 1  
 11111302 0.0 2  
 \* Initial temperature flag (see p.208 of Manual Appendix A)  
 11111400 0  
 \* Initial temperature; mesh point number  
 11111401 325.0 2  
 11111402 293.15 3  
 \* Left boundary condition definition (here: vol number); increment;  
 \* Boundary condition type (101: convection); surface area code (1: length);  
 \* Length; heat structure number  
 11111501 111010000 10000 101 1 9.5940e-2 6  
 11111502 111070000 10000 101 1 0.12662 12  
 \* Right boundary condition, see above (-30: T defined in general table 30; 1000: T set in Word 1)  
 11111601 -30 0 1000 1 9.5940e-2 6  
 11111602 -30 0 1000 1 0.12662 12  
 \* Power source (table number); internal source multiplier; direct mod heatin mult (left)  
 \* Direct mod heatin mult (right); heat structure number  
 11111701 0 0.0 0.0 0.0 12

\* Additional left boundary: heat transfer hydraulic diameter; heated length fwd (10.: ignore);  
 \* Heated length rev (10.: ignore); grid spacer length fwd (0.: ignore); grid spacer length rev (0.: ignore);  
 \* Grid loss coef fwd (0.: ignore); grid loss coef rev (0.: ignore); boiling factor (1.: subcooled liquid);  
 \* Heat structure number  
 1111801 0.0 10.0 10.0 0.0 0.0 0.0 0.0 1.0 12  
 \*  
 \* Bottom of heater outer tube  
 \* Number of axial heat structures; number of radial mesh points;  
 \* Geometry type (2: cylindrical, coupled to hydrodynamic component);  
 \* Steady-state initialization flag (1: initial T calculated by code);  
 \* Left boundary coordinate; reflood condition  
 11112000 4 3 2 1 0.009135 0  
 \* Mesh location flag; mesh format flag (see p.207 of Manual Appendix A)  
 11112100 0 1  
 \* Number of intervals; right coordinate  
 11112101 1 0.0127  
 11112102 1 0.0889  
 \* Composition (table number); interval number  
 11112201 100 1  
 11112202 120 2  
 \* Power input proportion; mesh interval number  
 11112301 1.0 1  
 11112302 0.0 2  
 \* Initial temperature flag (see p.208 of Manual Appendix A)  
 11112400 0  
 \* Initial temperature; mesh point number  
 11112401 325.0 2  
 11112402 293.15 3  
 \* Left boundary condition definition (here: vol number); increment;  
 \* Boundary condition type (101: convection); surface area code (1: length);  
 \* Length; heat structure number  
 11112501 111130000 10000 101 1 0.0400625 4  
 \* Right boundary condition, see above (-30: T defined in general table 30; 1000: T set in Word 1)  
 11112601 -30 0 1000 1 0.0400625 4  
 \* Power source (table number); internal source multiplier; direct mod heatin mult (left)  
 \* Direct mod heatin mult (right); heat structure number  
 11112701 0 0.0 0.0 0.0 4

\* Additional left boundary: heat transfer hydraulic diameter; heated length fwd (10.: ignore);  
 \* Heated length rev (10.: ignore); grid spacer length fwd (0.: ignore); grid spacer length rev (0.: ignore);  
 \* Grid loss coef fwd (0.: ignore); grid loss coef rev (0.: ignore); boiling factor (1.: subcooled liquid);  
 \* Heat structure number  
 11112801 0.006904 10.0 10.0 0.0 0.0 0.0 0.0 1.0 4  
 \*  
 \* Bottom of heater inner tube  
 \* Number of axial heat structures; number of radial mesh points;  
 \* Geometry type (2: cylindrical, coupled to hydrodynamic component);  
 \* Steady-state initialization flag (1: initial T calculated by code);  
 \* Left boundary coordinate (schedule 40 stainless steel); reflood condition  
 11113000 4 2 2 1 0.004623 0  
 \* Mesh location flag; mesh format flag (see p.207 of Manual Appendix A)  
 11113100 0 1  
 \* Number of intervals; right coordinate  
 11113101 1 0.007205  
 \* Composition (table number); interval number  
 11113201 100 1  
 \* Power input proportion; mesh interval number  
 11113301 1.0 1  
 \* Initial temperature flag (see p.208 of Manual Appendix A)  
 11113400 0  
 \* Initial temperature; mesh point number  
 11113401 325.0 2  
 \* Left boundary condition definition (0: adiabatic); increment;  
 \* Boundary condition type (0: adiabatic); surface area code (1: length);  
 \* Length; heat structure number  
 11113501 0 0 0 1 0.0400625 4  
 \* Right boundary condition, see above (101: convection)  
 11113601 111130000 10000 101 1 0.0400625 4  
 \* Power source (no source); internal source multiplier; direct mod heatin mult (left)  
 \* Direct mod heatin mult (right); heat structure number  
 11113701 0 0.0 0.0 0.0 4  
 \* Additional right boundary: heat transfer hydraulic diameter; heated length fwd (10.: ignore);

\* Heated length rev (10.: ignore); grid spacer length fwd (0.: ignore); grid spacer length rev (0.: ignore);

\* Grid loss coef fwd (0.: ignore); grid loss coef rev (0.: ignore); boiling factor (1.: subcooled liquid);

\* Heat structure number

11113901 0.008754 10.0 10.0 0.0 0.0 0.0 0.0 1.0 4

\*

\*\*\*\*\*

\* Material properties

\*\*\*\*\*

\*

\* Stainless steel

\* Material type (user supplied table); thermal conductivity format flag;

\* Volumetric heat capacity format flag (see p.227 of Manual Appendix A)

20110000 tbl/fctn 1 1

\* Stainless steel thermal conductivity (T; k) from  $k=14.6+0.0127*T[^\circ C]$

\*

(<http://www.mace.manchester.ac.uk/project/research/structures/strucfire/>

\*

[materialInFire/Steel/StainlessSteel/thermalProperties.htm](http://www.mace.manchester.ac.uk/project/research/structures/strucfire/materialInFire/Steel/StainlessSteel/thermalProperties.htm)

20110001 250.0 14.31

20110002 300.0 14.94

20110003 350.0 15.58

20110004 400.0 16.21

20110005 450.0 16.85

20110006 500.0 17.48

20110007 700.0 20.02

20110008 1000.0 23.83

\* Stainless steel volumetric heat capacity (T; rho\*cp)

\* From  $cp=450+0.28*T[^\circ C]-2.91E-4*T[^\circ C]^2+1.34E-7*T[^\circ C]^3$  (same source)

\* and  $\rho=8030[kg/m^3]$

(<http://www.lenntech.com/stainless-steel-304.htm>)

20110051 250.0 3.56e6

20110052 300.0 3.67e6

20110053 350.0 3.77e6

20110054 400.0 3.86e6

20110055 450.0 3.94e6

20110056 500.0 4.02e6

20110057 700.0 4.23e6

20110058 1000.0 4.43e6

\*

\* Copper

\* Material type (user supplied table); thermal conductivity format flag;

\* Volumetric heat capacity format flag (see p.227 of Manual Appendix A)

20111000 tbl/fctn 1 1

\* Copper thermal conductivity (T; k)

\* From

[http://www.efunda.com/materials/elements/TC\\_Table.cfm?Element\\_ID=Cu](http://www.efunda.com/materials/elements/TC_Table.cfm?Element_ID=Cu)

20111001 250.0 406.

20111002 300.0 401.

20111003 350.0 396.

20111004 400.0 393.

20111005 500.0 386.

20111006 1000.0 352.

\* Copper volumetric heat capacity (T; rho\*cp)

\* cp from

[http://www.efunda.com/materials/elements/HC\\_Table.cfm?Element\\_ID=Cu](http://www.efunda.com/materials/elements/HC_Table.cfm?Element_ID=Cu)

\*  $\rho=8940[kg/m^3]$

20111051 200.0 3.18e6

20111052 250.0 3.34e6

20111053 298.15 3.44e6

20111054 350.0 3.51e6

20111055 400.0 3.56e6

20111056 500.0 3.64e6

20111057 600.0 3.73e6

\*

\* Fiberglass insulation

\* Material type (user supplied table); thermal conductivity format flag;

\* Volumetric heat capacity format flag (see p.227 of Manual Appendix A)

20112000 tbl/fctn 1 1

\* Fiberglass insulation thermal conductivity (T; k) from  $k=7.702E-4*T[^\circ C]+0.206$

\* (CIET-DESIGN-

141\_Properties\_PSHT2\_Materials)

20112001 250.0 0.172766

20112002 293.15 0.221404

20112003 350.0 0.249786

20112004 400.0 0.288296

20112005 500.0 0.365316

20112006 600.0 0.442336

\* Fiberglass insulation volumetric heat capacity (T; rho\*cp)

\* From  $cp=844[J/kg-K]$  and  $\rho=20[kg/m^3]$

20112051 250.0 1.69e4

20112052 293.15 1.69e4

20112053 350.0 1.69e4

20112054 400.0 1.69e4

20112055 500.0 1.69e4

20112056 600.0 1.69e4

\*

\*\*\*\*\*

\* General tables

\*\*\*\*\*

\*

\* Heater power  
\* Table type  
20201000 power  
\* Time; power [W]  
20201001 0.00000 1707.0  
20201002 20000.0 1707.0  
\*  
\* HX surface temperature  
\* Table type  
20202000 temp  
\* Time; temperature [K]  
20202001 0.00000 298.15  
20202002 20000.0 298.15  
\*  
\* Ambient temperature  
\* Table type  
20203000 temp  
\* Time; temperature [K]  
20203001 0.00000 293.15  
20203002 20000.0 293.15  
\* End of input  
.